



OPERATIONAL SERVICES BRANCH

ENGINEERING LABORATORY REPORT

LP188/2013

Dynamic Simulation and Derailment Forces Analysis

Montreal, Maine & Atlantic Railway, Train MMA-002

Date of Occurrence: 06-Jul-2013

ATTENTION:

CROWN COPYRIGHT. THIS REPORT IS RELEASED FOR SAFETY PURPOSES ONLY, AND MAY BE AMENDED PRIOR TO, OR SUBSEQUENT TO RELEASE OF THE FINAL TSB REPORT. REPRODUCTION OF THIS DOCUMENT, IN WHOLE OR IN PART, MAY BE PERMITTED ON REQUEST TO THE TSB.

OCCURRENCE NUMBER	OCCURRENCE CLASSIFICATION	NUMBER OF PAGES	NUMBER OF APPENDICES	RELEASE OUTSIDE THE TSB REQUIRES REVIEW BY THE ACCESS TO INFORMATION AND PRIVACY OFFICE.	YES	NO
R13D0054	2	38	3		<input checked="" type="checkbox"/>	<input type="checkbox"/>

PREPARED BY

Daoxing Chen

D. Chen, Ph.D. (Senior Engineer Specialist - Rail Dynamics)

APPROVED BY

T. Givins

T. Givins, P.Eng. (Manager, Recorder and Vehicle Performance)

RELEASED BY

L. Donati

L. Donati, Ph.D. (Director of Operational Services)

RELEASED ON

9 APR 2014

REVISION

Table of Contents:

1.0	INTRODUCTION	1
1.1	Description of Occurrence	1
1.2	Background.....	1
1.3	Engineering Services Requested.....	2
2.0	CENTRIFUGAL FORCE AND ROLLOVER SPEED AT POD CURVE.....	3
2.1	Equilibrium Speed and Superelevation.....	3
2.2	Lateral Forces on Curve.....	4
2.3	Rollover Speeds at POD Curve.....	5
3.0	SIMULATION OF IN-TRAIN FORCE.....	6
3.1	Train Dynamic Model and Parameters	6
3.2	Dynamic Equilibrium Equations and Solution	7
3.3	Coupler/Draft Gear Elements	8
3.4	Air Brake Systems	8
3.5	Drag Resistance	9
3.6	Curve and Grade Resistance	10
3.7	Special Conditions	10
3.8	Transformed Lateral Force and L/V Ratio.....	10
4.0	VAMPIRE VEHICLE/TRACK DYNAMIC SIMULATION.....	12
4.1	Track Geometry Irregularities.....	12
4.2	Vehicle/Track Dynamic Model.....	13
4.3	Simulation Case Design.....	15
5.0	ANALYSIS.....	16
5.1	Rollover Speeds	16
5.2	Lateral Forces from Centrifugal Force	16
5.3	Simulated In-train Force	17
5.4	Transformed Lateral Forces from In-train Force	18
5.5	Combination of Centrifugal Force and In-train Force	19
5.6	Vampire Simulation Results	20
6.0	CONCLUSIONS.....	23
7.0	REFERENCES	24

List of Tables:

Table 1: Equivalent Lateral Force and Roll Moment on Car Model	14
Table 2: Simulation Cases and Parameters.....	15
Table 3: Calculated Rollover Speeds Due to Centrifugal Force.....	16
Table 4: Lateral Forces and Unloading Induced by Centrifugal Force	17
Table 5: Simulated In-train Buff Force and Transformed Lateral Forces	18
Table 6: Combined Lateral Forces and Unloading	20
Table 7: Simulated Derailment Indicators around the POD	21

List of Figures:

Figure 1: Aerial View of Derailment Site.....	25
Figure 2: Train Weight Profile.....	25
Figure 3: Centrifugal Force and Rollover Condition on Curve	26
Figure 4: Longitudinal Forces on Sample Vehicle Model.....	26
Figure 5: Coupler/Draft Gear Model	27
Figure 6: Grades and Curves in the Simulation Section.....	27
Figure 7: Grades of the Simulation Section around the POD.....	28
Figure 8: Simulated In-Train Force Distribution at the Derailment Moment.....	28
Figure 9: Schematic of Aligned Car Rollover	29
Figure 10: Forces on a Jack-knifed Car	29
Figure 11: Track Geometry Brush Chart on 21 August 2012.....	30
Figure 12: Curve and Switch Track Section with Depressed Rail Joint Defects.....	30
Figure 13: Breakdown of In-train Force on Vampire Vehicle Model	31
Figure 14: Wheel L/V Ratios in Case 1: MeasuredTrack_9DegF100V65	31
Figure 15: Wheel Loading Percentage in Case 1: MeasuredTrack_9DegF100V65	32
Figure 16: Wheel L/V Ratios in Case 2: MeasuredTrack_1p26DegF100V65	32
Figure 17: Wheel Loading Percentage in Case 2: MeasuredTrack_1p26DegF100V65... ..	33
Figure 18: Wheel L/V Ratios in Case 3: MeasuredTrack_NoForceV65	33
Figure 19: Wheel Loading Percentage in Case 3: MeasuredTrack_NoForceV65.....	34
Figure 20: Wheel L/V Ratios in Case 4: MeasuredTrack_9DegF100V30	34
Figure 21: Wheel Loading Percentage in Case 4: MeasuredTrack_9DegF100V30.....	35
Figure 22: Wheel L/V Ratios in Case 5: IdealCurve_9DegF100V65	35
Figure 23: Wheel Loading Percentage in Case 5: IdealCurve_9DegF100V65	36
Figure 24: Wheel L/V Ratios in Case 6: IdealCurve_1p26DegF100V65	36
Figure 25: Wheel Loading Percentage in Case 6: IdealCurve_1p26DegF100V65	37
Figure 26: Wheel L/V Ratios in Case 8: TrackGeomOnly_NoCurve_NoFV65	37
Figure 27: Wheel Loading Percentage in Case 8: TrackGeomOnly_NoCurve_NoFV65	38
Figure 28: Sample Lateral Force of Left Lead Wheel in Case 1, 2 and 4	38

List of Appendices:

Appendix A: Track Geometry Defects around the POD Section.....	A-1
Appendix B: UMLER Data of Sample Tank Cars	B-1
Appendix C: Summary of Vampire Simulation Results	C-1

1.0 INTRODUCTION

1.1 Description of Occurrence

1.1.1 On 06 July 2013, shortly before 0100 Eastern Daylight Time, eastward Montreal, Maine & Atlantic Railway freight train No. 2, which had been parked unattended for the night at Nantes, Quebec, started to roll uncontrolled. The train travelled a distance of about 7.2 miles, reaching a speed of 65 mph. At about 0115, while approaching the centre of the town of Lac-Mégantic, Quebec, 63 tank cars carrying petroleum crude oil, UN 1267, and 1 box car derailed. As a result of the derailment, about 6 million litres of petroleum crude oil spilled. There were fires and explosions, which destroyed 40 buildings, 50 vehicles and the railway tracks at the west end of Megantic Yard. A total of 47 people were fatally injured.

1.1.2 Preliminary examination of the derailment site determined that buffer box car CIBX 172032, immediately behind the locomotive consist, and the following 63 loaded tank cars derailed on the main track of a 4.25° right-hand curve in the direction of travel (eastward), covering a No. 11 turnout. The locomotive consist separated from the derailed cars and split into 2 portions, with each travelling different distances before they came to a stop. After a significant time, the front portion of the locomotive consist moved backward (westward) and collided with the second portion, both moving a short distance further (westward) and coming to a final stop together.

1.1.3 The derailed buffer box car struck a stationary cut of cars on the siding track. The following 8 tank cars were scattered in separated jackknifed positions. The next 2 tank cars lay in the direction of the turnout siding, ahead of the main jackknifed pile-up of the rest of the derailed tank cars among which the fire and explosions occurred. The last 9 tank cars in the train did not derail. They were disconnected and removed back and away from the derailment and fire by the locomotive engineer and emergency responders. An aerial-view photograph of the accident site is shown in Figure 1.

1.2 Background

1.2.1 Train MMA-002 consisted of 5 locomotives, 1 operation control car VB-1, 1 loaded buffer box car, and 72 tank cars loaded with petroleum crude oil. The train weighed 10 287 tons and was 4701 feet long. The train weight profile is shown in Figure 2.

1.2.2 The train was operated by a 1-person crew. Before midnight, it came to a stop on the main track of Station Nantes with an automatic application of the air brakes. The locomotive engineer applied hand brakes on the locomotive consist and the buffer car, and then released the automatic brake, but kept the independent brake (IND) of the locomotive consist in the applied position. The engine of the lead locomotive, MMA 5017, was kept running at idle to maintain the air brake supply. The locomotive engineer left the train and went to a hotel for rest, as indicated in his schedule.

- 1.2.3 A fire was detected on the lead locomotive sometime after the locomotive engineer left (LP181/2013). Local firefighters came and put out the fire. A local MMA engineering employee was called to attend to the fire site. The engine of the locomotive was shut down, and the train was left unattended again. Approximately 59 minutes later, the train started to move down the descending grades, and accelerated all the way until it reached the town of Lac-Mégantic, where it derailed.
- 1.2.4 The lead locomotive, MMA 5017, was equipped with a Quantum Engineering Incorporated (QEI) locomotive event recorder (LER) version no. S45E, serial no. 0204100033. The recorded data in the “extend log” was downloaded from MMA 5017 by a MMA staff member soon after the accident and provided to the TSB.
- 1.2.5 The train was also equipped with an end-of-train (EOT) sense and brake unit (SBU). The SBU was sent to the TSB Engineering Laboratory for examination (LP 132/2013). The records in the DataFlash were extracted and converted into Excel spreadsheets. The EOT SBU download data were provided for a comprehensive analysis of LER and SBU data together.
- 1.2.6 The TSB investigation team also obtained a copy of the standard report of the public crossing at Mile 117.11, Moosehead Subdivision, that indicated the activation of the crossing signal and protection. The time record was calibrated by an independent crossing company. This record was used as a reference in the synchronization and calibration of the downloaded LER time records. The comprehensive analysis of the downloaded LER records, SBU data and the standard report of the public crossing at Mile 117.11 was conducted and a number of significant events of interest were identified to assist the investigation (LP136/2013).
- 1.3 Engineering Services Requested
- 1.3.1 The preliminary investigation found that the train experienced a number of events, including unattended parking, fire, engine shutdown, runaway, derailment, and explosion. There were several broken knuckles, including those between the second and third locomotives, indicating that the locomotive consist had separated and rejoined. The derailed cars were scattered in several small, jackknifed groups as well as in a main pile-up. The final positions of the derailed cars and the LER data analysis suggested that the point of derailment (POD) was likely located around the west end switch on the 4.25⁰ right hand curve. The excessive centrifugal force due to the high speed (65 mph at the derailment) may have caused or contributed to the derailment.
- 1.3.2 A laboratory project was opened for calculation of the lateral force and the rollover speed at the POD curve. The preliminary calculation indicated that the derailment speed was lower than the rollover speed due to the pure centrifugal force on the curve for the derailed tank cars. A further simulation was conducted to obtain the longitudinal in-train force at the derailment moment and the corresponding transformed lateral force. The combination of the centrifugal force and the transformed lateral force of the in-train buff force could cause the derailment if the couplers and the tank car were in jackknifed position.

- 1.3.3 Subsequently, the investigation team obtained the latest track geometry car test records in form of brush charts dated 21 August, 2012 which showed some significant geometry irregularities near the switch. These track geometry defects might generate significant dynamic forces and contribute to the derailment. However, the digital data of the track geometry record charts was not available and the track geometry state on the day of occurrence was not known as the track was destroyed in the accident. It is not possible to determine the exact effect of the track geometry condition and the resulting dynamic force quantitatively.
- 1.3.4 The TÜV Rheinland Mobility Inc. Rail Sciences Division (TRRSI) was contracted to conduct a Vampire vehicle/track dynamic simulation to evaluate the effect of the track geometry. A generalized tank car model developed by TRRSI was used. As the track and derailed cars were destroyed, it was not possible to obtain the actual wheel and rail profiles of the first derailed car at the POD. Standard AAR wheel and rail profiles were used in the simulation.
- 1.3.5 This LP report describes the calculation of the centrifugal force on the curve caused by the high speed, the simulated in-train force at the derailment moment, the available track geometry records and Vampire simulated dynamic response. The analysis of the combination of the centrifugal force, the dynamic forces generated by the track geometry and the in-train force helps to identify and explain the most likely derailment scenario and the contributions of the factors.

2.0 CENTRIFUGAL FORCE AND ROLLOVER SPEED AT POD CURVE

2.1 Equilibrium Speed and Superelevation

- 2.1.1 Curved tracks are normally elevated by an amount (superelevation) depending on curvature to provide a lateral force balance at a given speed. The superelevation is the height, in inches, that the outer (high) rail of a curve is elevated above the inner (low) rail. It is intended to balance the effect of centrifugal force.
- 2.1.2 The weight of the vehicle, acting downward vertically from the vehicle's center of gravity (CG), is added to centrifugal force to create a resultant force as shown in Figure 3:
- A resultant force F that passes through the track centerline indicates balanced elevation and the weight of the vehicle will be distributed equally between the high and low rails.
 - A resultant that passes to the inside of track centerline indicates over-balanced elevation.
 - A resultant that passes to the outside of the track centerline indicates under-balanced elevation.

- 2.1.3 The equilibrium speed on a curve is the speed at which the resultant of the weight and the centrifugal force is perpendicular to the plane of the track. The relationship is

$$h_b = 0.0007DV^2$$

where h_b is balance superelevation, inches
 D is degree of curvature (100-foot chord)
 V is train speed, mph

- 2.1.4 The MMA requires that the maximum allowable operating speed for each curve must not produce an underbalance in excess of 1 ½ inches unless authorized by the System Office of Engineering. The maximum speed will be computed using the following formula:

$$V_{\max} = \text{sqrt} [(h_a + u) / (0.0007D)]$$

Where V_{\max} is maximum allowable operating speed, mph
 h_a is actual elevation of the outer rail, inches
 u is underbalance, inches
 D is degree of curvature

- 2.1.5 The average superelevation in the 4.25° curve located from Mile 0.05 to Mile 0.28 was about 1 ½ inches, corresponding to a balanced speed of 22 mph. Typically, for freight trains negotiating this degree of curvature with the superelevation that existed, train speed should not exceed 32 mph (assuming a maximum of 1 ½ inches of underbalance).

2.2 Lateral Forces on Curve

- 2.2.1 A rail vehicle travelling on a curved track at a speed generates a centrifugal force, as shown in Figure 3. The centrifugal force F_{cg} can be calculated as:

$$F_{cg} = (W / g) * V^2 / R$$

$$R = 5730 / D$$

where W is the gravity force or weight, in lbs
 g is the gravity acceleration or gravitational constant, 32.16 ft/s/s
 V is the speed at curve, feet/sec
 R is the radius of curve, in feet
 D is the degrees of curve

- 2.2.2 The centrifugal force F_{cg} acts at the center of gravity of the vehicle in the lateral outward direction and transmits to the wheel/rail interface. The elevation h on the curve transforms a portion of the vehicle weight into a lateral inward force L_e .

$$L_e = W * \tan (\alpha_1) = W * h / B$$

where α_1 is the elevation angle, rad

h is the superelevation, inches

B is the track width between rail centers, approximately 59 inches.

- 2.2.3 The net lateral force on the entire car L_c is the balance of the centrifugal force and the lateral portion of weight due to elevation.

$$L_c = F_{cg} - L_e$$

- 2.2.4 The vertical forces on the outer rail V_{out} and the inner rail V_{in} are respectively

$$V_{out} = W/2 + F_{cg} * H/B$$

$$V_{in} = W/2 - F_{cg} * H/B$$

where H is the height of center of gravity of vehicle above rail top, in inches

- 2.2.5 The lateral force of the entire vehicle on the outer rail is

$$L_{out} = L_c - V_{in} * f$$

where f is coefficient of friction between wheel tread and rail top

- 2.2.6 The lateral forces of a truck side, a wheel on the outer rail and an axle are approximately,

$$\text{truck side} \quad L_{ts} = L_{out}/2$$

$$\text{wheel} \quad L_w = L_{out}/4$$

$$\text{axle} \quad L_{ax} = L_c /4$$

2.3 Rollover Speeds at POD Curve

- 2.3.1 Vehicles may roll over outward on curves at high speeds because of excessive centrifugal force, as shown in Figure 3. The critical condition occurs when the compound force F resulting from the centrifugal force F_{cg} and the gravity force W points to the high (outer) rail so the low (inner) wheel will be lifted from the low rail. Under the critical condition, the following equation exists:

$$\tan(\alpha) = \tan(\alpha_1 + \alpha_2) = F_{cg} / W$$

$$\alpha_1 = \tan^{-1}(h/B)$$

$$\alpha_2 = \tan^{-1}(B/2/H)$$

where h is the elevation on curve, in inches

B is the track width between rail centers, inches

H is the height of center of gravity of vehicle above rail top, in inches

2.3.2 The critical rollover speed V_r can be calculated as

$$F_{cg} / W = (W / g) * V_r^2 / R / W = V_r^2 / (g R) = \tan (\alpha)$$

$$V_r^2 = (g R) \tan (\alpha)$$

$$V_r = \text{sqrt} [(g R) \tan (\alpha)]$$

3.0 SIMULATION OF IN-TRAIN FORCE

3.1 Train Dynamic Model and Parameters

3.1.1 A longitudinal dynamic model of a train consists of any combination of a number of different locomotives and a large number of different cars. Only one locomotive (normally the lead one) takes operational control, while the other locomotives, which can be located anywhere within the train, will act according to the control orders from the control locomotive. Cars are passive bodies subject to dynamic rules and application of traction, dynamic brake (DB) and air brake forces according to the response output of their air brake systems with respect to trigger times and air pressures.

3.1.2 Every vehicle, including the locomotives and cars, is modeled as a rigid body with a mass and length that is supported vertically by trucks and wheel axles, with a draft gear at each end of the body, and connected by a pair of couplers between the draft gears of the adjoining vehicles according to the train consist.

3.1.3 The parameters for each vehicle include:

- order number (from the front to the rear of the train),
- mass (or weight),
- tare weight (light weight, for calculation of brake force),
- length,
- longitudinal location X_0 of the front end at simulation start time,
- air brake system type and parameters (braking ratio, friction coefficient etc.), for each car,
- front draft gear type/initial position,
- rear draft gear type/initial position, and
- ratio of air pipeline length to vehicle length.

3.1.4 Additional parameters for locomotives include:

- traction force chart by throttle levels and speed,
- dynamic braking force chart by DBN and speed, and
- independent braking force state (bail on/off).

3.1.5 Conditions and parameters for the whole train include:

- operation activities in time or mileage series (throttle levels, dynamic braking, emergency braking, brake air pressure, bail independent brake etc.).
- track grades in mileage series.

- track curvatures in mileage series.
- initial speed and acceleration (time history as a reference), and
- other initial and boundary conditions.

3.2 Dynamic Equilibrium Equations and Solution

3.2.1 A model of a sample vehicle in the train with all applying forces is shown in Figure 4, and its dynamic equilibrium equations are established according to mathematics and dynamics rules.

3.2.2 Forces acting on each vehicle include:

- inertia forces (acceleration times mass) F_a ,
- air brake forces (on each vehicle as a whole, the output of its air brake system with a trigger time and propagation distance) F_b ,
- drawbar forces or in-train force (function of relative displacement and velocity of the adjoining vehicles) F_{bf} or F_{in} ,
- drag resistance including air resistance (function of speed) and adjust resistance F_{dr} ,
- curve resistance (function of speed, curvature) F_{cr} , and
- grade resistance (function of grade) F_{gr} .

3.2.3 Among the above forces, air brake forces and drawbar forces are the most complex functions involving multiple non-linear parameters. It is conventional and more convenient to model them as black box subsystems, and to establish their detailed models in respective libraries of air brake systems and draft gear systems. For each type of air brake subsystem, or pair of draft gears, a sub model is used to establish a nonlinear input-output function.

3.2.4 Additional forces on locomotives include:

- DB forces (function of speed and DB level, given by locomotive manufacturers, or from LER records), and
- traction forces (function of speed and throttle levels, given by manufacturers, or from LER records).

3.2.5 Dynamic equilibrium condition: The dynamic equilibrium of all forces was established for each vehicle and assembled for the whole train by setting the draft gear force between the adjoining vehicles the same.

3.2.6 Friction limit condition: All braking or traction forces on a vehicle could not exceed the maximum friction force determined by the friction between wheel and rail, $F_b \leq f * W_t$, where f is friction coefficient and W_t is the tare weight.

3.2.7 Boundary conditions: The drawbar force of the front draft gear of the lead locomotive, and that of the rear draft gear of the last vehicle were zero, $F_{bf}(0) = F_{bf}(N) = 0$, where N is the total number of vehicles in the train including locomotives.

3.2.8 Initial condition: A set of designated values were set up at the start moment for the system variable vectors to run a designated procedure.

- 3.2.9 Dynamic differential equations for the longitudinal location $X(t)$ of the front end (or center) of each vehicle at time t were established. The equations are nonlinear second order differential equations.
- 3.2.10 A number of direct time integration algorithms were available to solve the nonlinear differential equations. The integration time step is an important parameter that requires careful selection in order to reach a stable and accurate solution.
- 3.2.11 Other associated variables that can be calculated and outputted from the solved basic variables are:
- dynamic displacement, velocity, and acceleration/deceleration of each vehicle,
 - drawbar force at each draft gear (distribution along the train),
 - maximum drawbar force in the train,
 - brake distance,
 - energy consumption, and
 - propagation of air braking along the train line

3.3 Coupler/Draft Gear Elements

- 3.3.1 The coupler/draft gear elements between adjoining vehicles are one of the two most complex nonlinear elements (the other is the air brake elements) in train dynamics models. Adjoining vehicles are connected by the coupler/draft gear elements that consist of a coupler and a draft gear from each of the two adjoining vehicles. The coupler is regarded as a rigid body and its mass is ignored, while the draft gear possesses a nonlinear relationship between the draft gear relative movement and its reaction force.
- 3.3.2 As the couplers are connected and the forces on each of them are equal, the coupler/draft gear elements between two adjoining cars can be modeled separately or as a whole system converted into a black box with a compound nonlinear relationship between the inputs (relative movement of the adjoining vehicles) and the output (the equal drawbar force or coupler force), $F_{bf} = f_l(X_i, X_{i+1}, V_i, V_{i+1})$ as shown in Figure 5.
- 3.3.3 These black box elements can be established according to the actual pair of draft gears that are involved in the coupler/draft gear subsystem between the adjoining vehicles. The pair of draft gears from the adjoining vehicles might be identical or of different types. The conventional and most efficient method for modeling of black box elements is to establish a library of black box models corresponding to the commonly used draft gears.

3.4 Air Brake Systems

- 3.4.1 Air brake elements are another type of nonlinear, complex elements in train dynamics models. Similarly we can model them by nonlinear black box elements. The relationship between the input and output is also compound nonlinear, but could be simplified as a series of linear sections.
- 3.4.2 Air brake application or in-train initiated emergency (UDE) air braking are initiated and the brake signal propagates along the train. In the UDE case, after

the UDE signal arrives in the locomotives, the train information and braking system (TIBS), if equipped, initiates the end of train (EOT) emergency braking with an approximate 2 second delay.

- 3.4.3 At each vehicle in the train, once the air brake signal arrives, the brake pipe pressure (BP) starts to drop and reaches zero. Then brake cylinder pressure (BC) starts to build up and reaches the maximum level in a time T_b . The BC pressure pushes the brake shoes to apply a brake shoe force on the wheel. The retarding braking force F_b can be expressed as:

$$F_b = R_b * W * f * BC / BC_{max}$$

Where R_b is the braking ratio

W is the weight

f is the coefficient of friction

BC is the brake cylinder air pressure

- 3.4.4 The BC pressures at the vehicles in the train are calculated based on the locations of the vehicles, initiation origin and mechanism, braking signal propagation rate along the train and BC build up time, T_b . With the TIBS system and activation delay, the emergency braking could be initiated from both the locomotives and the EOT to reduce the propagation time and build up BC along the train in a shorter time. This also helps reduce braking force differences and in-train forces due to the propagation delay.

3.5 Drag Resistance

- 3.5.1 Drag resistance force on a train includes air resistance, which is a function of speed, and friction resistance, such as that of roller bearings and wheel/track interface. Experiments have shown that drag resistance force is proportional to the weight of vehicles or train.

$$F_{dr} = R_{dr} * W$$

- 3.5.2 The drag resistance coefficient R_{dr} is expressed as resistance per unit weight. Several tests have resulted in experimental formulas to calculate the unit drag resistance, among which the Davis equation [1][2] is most commonly used:

$$R_D = 1.3 + 29/w + B * V + C * A * V^2 / W$$

$$R_{dr} = K * R_D$$

Where R_D is the drag resistance coefficient by the Davis equation

w is weight per axle in tons

W is weight of the vehicle in tons

V is train speed in mph

A is the cross section area in square feet of the vehicle

B, C are experimental coefficients in Table 6.2 in [1]

K is an adjustment factor

3.6 Curve and Grade Resistance

3.6.1 Extra resistance occurs on curves and applies forces to the train. Curve resistance force F_{cr} is also a function of the weight of the vehicles.

$$F_{cr} = f_{cr} * D * W$$

3.6.2 The curve resistance coefficient f_{cr} is about 0.8 lb/ton/degree based on tests.

3.6.3 Extra forces are applied to a train when it runs on a grade slope. In the travel direction, a descent grade will add a grade force forward, and an uphill grade will add additional resistance force. The grade force F_{gr} is proportional to the weight of the vehicles and the grade.

$$F_{gr} = \text{sign}(\text{grade}) f_{gr} * G * W$$

3.6.4 The grade force, F_{gr} is assumed to be a resistance so sign (grade) takes a positive value for an uphill grade and a negative value for a descent grade in the travel direction. The coefficient f_{gr} is 20 lbs/ton/percent grade.

3.7 Special Conditions

3.7.1 The simulation focused on the runaway of Train MMA-002 up to the derailment moment. Only residual independent (IND) air brake was applied on the locomotives and hand brakes were applied on the locomotive consist and the buffer box car. This condition simplified the simulation.

3.7.2 The LER system recorded the runaway started when the IND dropped to 27 psi and the derailment occurred when the IND dropped to 16 psi and the train speed reached 65 mph. The track grades and curvatures were estimated from the track profile diagram in Figures 6 and 7. The difference between the model and the actual train was expressed by the adjustment factor to the drag resistance K , which was determined by comparison of the simulated speed and the LER records in the most likely case, and this adjustment factor was applied to all simulation cases.

3.7.3 The simulated in-train force distribution along the train at the derailment moment is plotted in Figure 8. The maximum in-train force appeared at car No. 10 from the train head end which located at the transition from grade 1.2% to the nearly flat terrain. The front tank cars (No. 3 to No.10 in train consist) at the highest in-train forces were located at the vulnerable section of the switch on the curve where the POD and main pile-up were observed.

3.8 Transformed Lateral Force and L/V Ratio

3.8.1 Longitudinal in-train force, F_{in} is transformed into lateral force at the drawbar L_{bar} whenever the couplers take an angle against the longitudinal central line of the car body, called coupler angle or drawbar angle. The transformed lateral force L_{bar} is proportional to the sine of the drawbar angle α .

$$L_{bar} = F_{in} * \sin \alpha$$

- 3.8.2 When a train is in compression or buff state, particularly in a zigzag or jackknifed position, the drawbar angle can reach its maximum with the couplers pushing against the side of the housing. Longitudinal forces can be transformed into large lateral forces which can impact the truck and be transmitted to the rail. Excessive transformed lateral force can cause different types of derailments [3][4] depending on the positions of the involved cars and couplers and the track resistance. If the lateral ballast resistance against tie movement (panel shift) is stronger than the fastening constrain against rail rollover, the transformed lateral force can cause a car rollover, wheel climb or rail rollover derailment. Otherwise, it can cause track panel shift and lead to a different type of derailment.
- 3.8.3 If the car is in a horizontal alignment position as shown in Figure 9, the transformed lateral force L_{bar} at the drawbars of the car ends produce lateral force acting on the truck L_{tr} .

$$L_{\text{tr}} = L_{\text{bar}}$$

- 3.8.4 If the car is in a horizontal zigzag or jack-knifed position shown in Figure 10, the transformed lateral force L_{bar} at the drawbars of the car ends produce lateral force acting on the truck L_{tr} , which is L_{bar} times a ratio of car length l_c over truck centre l_{tc} .

$$L_{\text{tr}} = L_{\text{bar}} * l_c / l_{tc}$$

- 3.8.5 The transformed lateral force L_{tr} , at the truck can change the vertical forces on the rails. As the transformed lateral force acts at the coupler height above the rail top, the truck side vertical forces are changed into:

$$V_{\text{outts}} = W/4 + L_{\text{tr}} * H_c/B$$

$$V_{\text{ints}} = W/4 - L_{\text{tr}} * H_c/B$$

- 3.8.6 In a case that a truck rolls over the rail or a wheel climbs the rail, the wheels on the truck side rolling over the rail push the rail with the flanges while the wheels on the other side sit on top of rail without flange contact. The truck side lateral force L that causes rail roll over equals L_{tr} minus the friction force on the top of the rail on the other side,

$$L_{\text{ts}} = L_{\text{tr}} - V_{\text{ints}} * f$$

Where V is the truck side vertical load

f is the friction coefficient between the wheel tread and the rail top

- 3.8.7 With the simulated in-train buff force F_{in} , the transformed truck side lateral force L_{ts} and L/V ratio can be calculated by the above formulas. A friction coefficient of 0.315 was used in the calculations to cover the speed range of simulation.
- 3.8.8 Under high centrifugal force and buff in-train force, the two wheels of a truck side are more likely pushed against the rail evenly by the transformed lateral force from the truck center. Therefore, the transformed wheel L/V ratio and truck side L/V ratio are likely equal and the wheel lateral force L_w is likely half of the truck side lateral force L_{ts} .

4.0 VAMPIRE VEHICLE/TRACK DYNAMIC SIMULATION

4.1 Track Geometry Irregularities

- 4.1.1 As prescribed by the Track Safety Rules (TSR), the main track was last visually inspected by a track maintenance employee in a hi-rail vehicle on 05 July 2013. During that inspection, no exceptions were noted in the area of the derailment.
- 4.1.2 The track was tested annually for rail flaws and geometry defects. The last continuous testing for internal rail defects was performed on 19 September 2012. No results were obtained between Mile 46.00 and Mile 0.00, including the derailment area.
- 4.1.3 A track evaluation car performed a track geometry inspection on 21 August 2012. The inspection car generated a brush chart as shown in Figure 11. In the immediate area of the Frontenac public grade crossing and the Megantic West main-track turnout, the inspection identified several urgent defects related to spiral cross-level, alignment/rate of change, wide gauge, misalignment and design speed (see Appendix A). The photo of the track section approaching the switch in Figure 12 also showed a depressed rail joint and corresponding geometry defects. Minor repairs were made to improve track conditions; however, no permanent repairs were made, and a temporary slow order was put in place.
- 4.1.4 The historic Transport Canada inspection records of the curve and turnout section and the TSB post derailment examination of the track sections over approximately 30 miles on either side of the town of Lac-Mégantic observed excessive rail wear, loose track components and other defects. For example, on 24 July 2012, a TC Safety Officer inspected the main track between Mile 0.00 and Mile 42.00 of the Sherbrooke Subdivision and the Officer observed that the frog, guard rail and heel bolts were loose for the turnout at Megantic West. On 14 May 2013, a TC Safety Officer observed that the fastenings at the same turnout were not intact or maintained. Other recurring defects that were noted included corrugated, battered rail joints, crushed head rail (deformation) and ballast missing at various locations.
- 4.1.5 The track at the POD was destroyed in the accident and its condition on the day of the occurrence could not be determined. There was no digital data file available corresponding to the track inspection brush charts. No track geometry data was available to allow a detailed and accurate vehicle/track dynamic simulation to quantitatively evaluate the effect of the track geometry. However, it is reasonable to assume that the recurring defects corresponding to the battered rail joint in front of the switch very likely existed on the day of occurrence. As the speed limit around the curve was very low, the track geometry condition could have been at low level.
- 4.1.6 Based on the railway dynamics knowledge and industrial experience, track geometry defects at urgent or priority level could generate significant dynamic forces and a derailment risk. If the track geometry defects around the POD as shown in Figure 11 recurred, they could generate high transient dynamic forces. On the day of occurrence, the dynamic effects of the track geometry defects were added to the lateral force and unloading from the centrifugal force and the in-train

- force, contributing to the derailment. There is no doubt that the combination of the three factors induced the high lateral force and unloading that caused the derailment.
- 4.1.7 The previous sections have accurately calculated the contributions of the centrifugal force and in-train force. The centrifugal force or the in-train force alone was not sufficient to cause the derailment, and the combination of the centrifugal force and the in-train force under the all alignment train condition was still not enough to cause the derailment. But the combination of the centrifugal force and in-train force under coupler jack-knifing condition could generate high lateral force and unloading that would impose a derailment risk.
- 4.1.8 Though the track geometry data on the day of occurrence was not available, the brush chart from the latest track geometry inspection on 21 August 2012 could be used as a reference data to estimate the possible effect of track geometry in a nominal Vampire vehicle/track dynamic simulation.
- 4.2 Vehicle/Track Dynamic Model
- 4.2.1 The VAMPIRE vehicle dynamics simulations were conducted to investigate the effects of track geometry and in-train force at coupler action on vehicle/track interaction of a model of a tank car similar to those involved in the Lac-Megantic derailment.
- 4.2.2 The vehicle and track were modeled based upon the information collected by the TSB investigation team. The coupler forces were applied to the car body of the tank car model in accordance to the force magnitudes and coupler angles determined in the previous sections.
- 4.2.3 The tank car model was created based upon the UMLER, center of gravity and weight data collected from the sample tank cars TILX0000316547 and WFIX0000130608. The UMLER files are included in Appendix B.
- 4.2.4 The following summarizes some of the pertinent features for the tank car model:
- Car body center of gravity height above top of rail = 91”
 - Total vehicle weight = 128 tons
 - Truck center distance = 45’ 10”
 - Axle spacing = 70”
 - Wheel diameter = 36”
 - Long travel constant contact side bearings
 - AAR 1B WF wheel profile
 - AREA 115 rail profile
- 4.2.5 The coupler forces of 100 kips buff force at the two different coupler angles were broken down into equivalent lateral forces and roll moments and applied to the car body CG in simulations involving coupler forces as in Figure 13. This resultant lateral force L is negative and the roll moment M is positive with respect to the VAMPIRE coordinate system when traversing a right hand curve.

$$L = 2 F_{in} * \sin \alpha$$

$$M = 2 F_{in} * \sin \alpha * H$$

- 4.2.6 The resultant lateral force and roll moment applied to the car body center of gravity are calculated and listed in Table 1 at two coupler angles, 1.26 degrees and 9 degrees, the minimum and maximum on the curve, corresponding to the aligned and jack-knifed coupler position. But the car body was assumed in aligned position.

Table 1: Equivalent Lateral Force and Roll Moment on Car Model

Coupler Force F_{in} (kip)	Coupler Height (in)	Car Body CG Height (in)	Car Body CG Height above Couplers (in)	Coupler Angle (degrees)	Total Lateral Force Applied at CG (lb)	Total Roll Moment Applied at CG (lb-in)
100	34.5	91	56.5	9	31287	1767708
				1.26	4398	248480
Note	All forces and moments were constantly applied onto the car body CG					

- 4.2.7 The vehicles were traveling in the direction of descending milepost with respect to the provided brush chart images in Figure 11. The point of derailment occurred at the location indicated on a right hand curve, approximately 4.25 degrees, in the direction of travel. Points were read off the charts in the direction of descending milepost at increments of approximately 16.5 feet (0.1 mile divided by 32).

- 4.2.8 The following data was read at each increment:

- Curvature
- Super Elevation
- Gauge
- Left Alignment
- Right Alignment
- Left Surface
- Right Surface

- 4.2.9 The read points were processed into channels of a VAMPIRE Irregularity file using the following relationships:

- Distance = Distance
- Cross Level = Superelevation
- Curvature = Curvature
- Lateral Irregularity = Average of Left Alignment and Right Alignment
- Vertical Irregularity = Average of Left Surface and Right Surface
- Gauge = Gauge

- 4.2.10 Positive and negative was reversed for the curvature and superelevation data points with respect to the datum lines of the brush chart as the direction of travel

was in descending mileposts and a right hand VAMPIRE sign convention was used.

- 4.2.11 Other measurements' sign convention were unchanged relative to the zero line on the charts provided. The values above the datum were considered positive while values below the datum were considered negative.
- 4.2.12 The simulations started through a 1000 feet tangent track with no track geometry irregularities to minimize the transient effect of the applied constant in-train force, then went into the curved track section approaching to the POD. The POD is at distance 2189 for the VAMPIRE track files created from the brush charts.

4.3 Simulation Case Design

- 4.3.1 Seven simulation cases were designed and performed to investigate the effects of the three contribution factors and their combinations. An additional case was conducted to assess a low speed at which the resultant forces would not cause derailment. The simulation results were compared with the previous calculations of steady state centrifugal force and transformed lateral force from the in-train force. The analysis of the results and differences between the cases identified the effects and roles of the factors on the derailment. The conditions and parameters of the 8 simulation cases are listed in Table 2.

Table 2: Simulation Cases and Parameters

Case	Speed	Track Condition	In-train Force	Coupler Angle
1	65	As Measured from the Brush Charts	100 kips Buff	9 degrees
2	65	As Measured from the Brush Charts	100 kips Buff	1.26 degrees
3	65	As Measured from the Brush Charts	None	NA
4	30	As Measured from the Brush Charts	100 kips Buff	9 degrees
5	65	Ideal 4.25 Degree RH Curve with 1.5" Superelevation	100 kips Buff	9 degrees
6	65	Ideal 4.25 Degree RH Curve with 1.5" Superelevation	100 kips Buff	1.26 degrees
7	65	Ideal 4.25 Degree RH Curve with 1.5" Superelevation	None	NA
8	65	As Measured from Brush Charts but No Curvature	None	NA

- 4.3.2 Case 1 to 3 would identify the most likely derailment scenarios of three factors and the effect of the in-train force and coupler angle. Case 4 would show the comprehensive effect of the speed compared with Case 1. Case 5 to 7 would show the effect of the in-train force and coupler angle on the ideal 4.25 degree curve. Comparison between Case 1 to 3 and Case 5 to 7 respectively would show the difference caused by the measured track geometry on the curve. Case 8 would

demonstrate the dynamic response of the track geometry irregularities solely on tangent track.

- 4.3.3 The lateral and vertical dynamic forces from all wheels were output and the derailment related indicators such as wheel L/V ratios, unloading percentage, axle sum L/V ratios and truck side L/V ratios were output in statistic form. Spread sheet files for the basic statistic outputs for each of the simulations shown above are included in Appendix C. Reported results were filtered with a 15 Hz 4 pole low pass filter. These statistic outputs are centered around the reported POD and will be analyzed in next section.

5.0 ANALYSIS

5.1 Rollover Speeds

- 5.1.1 The LER data analysis and derailment site survey indicated that the suspected first derailed cars were the loaded tank cars among cars No. 3 to No.10 in the train consist. If the train speed exceeded or was close to the rollover speed of the vehicle on the curve, the first derailment might be caused purely by the centrifugal force in the form of car rollover at the POD on 4.25⁰ right hand curve (R = 1348 feet) with an average elevation of 1 1/2 inches (a maximum local elevation of 3 5/8 inches was detected in the track geometry inspection on 21 August, 2012). The heights of the center of gravity of the loaded tank cars were between 88.8 inches and 91 inches, as recorded in the UMLER data. The height of the center of gravity of the involved locomotives was approximately 72 inches. The rollover speeds for the tank car with the low and high center of gravity and the locomotives are calculated and listed in Table 3.

Table 3: Calculated Rollover Speeds Due to Centrifugal Force

Parameters\Vehicle		Tank Car A	Tank Car B	Locomotives
Curvature D	degrees	4.25 ⁰	4.25 ⁰	4.25 ⁰
Radius R	feet	1348	1348	1348
Superelevation h	inches	1 ½	1 ½	1 ½
Track width B	inches	59	59	59
Elevation angle α_1	rad	0.0254	0.0254	0.0254
CG height H	inches	88.8	91	72
CG angle α_2	rad	0.3207	0.3135	0.3889
Total angle $\alpha = \alpha_1 + \alpha_2$	rad	0.3461	0.3389	0.4143
Rollover V_r	ft/s	123.10	121.69	135.92
Rollover V_r	mph	83.9	83.0	92.7
Note	$V_r = \text{sqrt} [(g R) \tan (\alpha)]$ Gravity acceleration $g = 31.16 \text{ ft/s/s}$			

- 5.1.2 The calculated rollover speeds due to centrifugal force on the curve for the involved tank cars and locomotives are significantly higher than the derailment speed of 65 mph. This difference indicates that the centrifugal force on the curve at 65 mph alone could not roll over the vehicles as long as the track was intact.

5.2 Lateral Forces from Centrifugal Force

- 5.2.1 Though the centrifugal force alone was insufficient to roll over the vehicles on the curve at the derailment moment, it induced a large lateral force on the vehicles that caused vertical load shift to unbalance and increased lateral force onto the outer rail side while the vertical load on the inner rail was reduced. It is essential to calculate and examine the lateral forces from the centrifugal force against the track resistance.
- 5.2.2 The calculated lateral forces from the centrifugal force are listed in Table 4. Tank Car A represents the lowest CG height and Tank car B represents the highest CG height. The induced truck side, wheel and axle lateral force were within the track strength, and the unloading $\Delta V/V_0$ percentages (65%-67% for the tank cars and 53% for the locomotives) were in the acceptable range. The L/V ratio was very low as the lateral force and vertical force increased simultaneously. This further indicated that the centrifugal force alone would not cause the derailment if the track was intact.

Table 4: Lateral Forces and Unloading Induced by Centrifugal Force

Parameters\Vehicle		Tank Car A	Tank Car B	Locomotive	Comment
CG height H	in	88.8	91	72	entire car
F_{cg}	lb	55382	55382	84371	
L_e	lb	6508	6508	9915	
L_c	lb	48873	48873	74455	
V_{in}	lb	44646	42581	92039	
V_{out}	lb	211354	213419	297961	
L_{out}	lb	34810	35460	45463	
L_{ts}	lb	17405	17730	22731	truck
L_w	lb	8702	8865	7577	entire car
L_{ax}	lb	12218	12218	12409	
L/V_{out}		0.16	0.17	0.15	
L_c/W		0.19	0.19	0.19	
ΔV_1	lb	83354	85419	102961	
$\Delta V_1/V_0$	%	65	67	53	

5.3 Simulated In-train Force

- 5.3.1 The vehicles in the runaway train were subjected to the similar centrifugal forces at the same speed at the derailment moment, but the front portion of the train including the locomotive consist and a few cars passed the POD without derailling. This observation confirmed that the centrifugal force alone was not sufficient to roll over the vehicles. There must have been some other factors contributing to the derailment. In-train force was a very likely factor. The train had the residual independent brake and hand brake on the locomotive consist and the buffer box car applied and ran on a descending grade approaching the POD curve which was located on a near flat track section. A significant in-train buff force was inevitable at the track section at the derailment moment.
- 5.3.2 The measured residual IND and hand brake force (LP187/2013) were used in the simulation and calculations. The train dynamics simulation obtained the distribution of in-train buff force along the train at the derailment moment as

shown in Figure 8. The highest in-train forces appeared among car No.3 to No. 10 that were located around the POD section at the LER recorded derailment moment. The simulated in-train buff forces at these vehicles of interest are listed in Table 5. The simulated in-train forces were approximately 100 to 110 kips at the cars of interest. The in-train force in this range was not unusual.

Table 5: Simulated In-train Buff Force and Transformed Lateral Forces

Vehicle	F _{in}	L _{tr}	ΔV	ΔV/V ₀	L _{tr}	ΔV	ΔV/V ₀
	lb	lb	lb	%	lb	lb	%
		Position a: aligned coupler and aligned carbody			Position b: aligned coupler and jack-knifed carbody		
Last Loco	86983	1913	4666	2.4	3027	7383	3.8
Car #3	96373	2119	5168	4.1	2747	6700	5.3
Car #4	98136	2158	5263	4.1	2798	6824	5.4
Car #5	99899	2197	5359	4.2	2848	6946	5.5
Car #6	101662	2235	5451	4.3	2897	7066	5.6
Car #7	103436	2275	5549	4.3	2949	7193	5.6
Car #8	105199	2313	5641	4.4	2998	7312	5.8
Car #9	106950	2352	5737	4.6	3049	7437	5.9
Car #10	108713	2391	5832	4.6	3100	7561	6
		Position c: jackknifed coupler and aligned carbody			Position d: jack-knifed coupler and carbody		
Last Loco	86983	13607	33188	16.9	21531	52515	26.8
Car #3	96373	15076	36771	29	19544	47668	37.5
Car #4	98136	15352	37444	29.5	19902	48541	38.2
Car #5	99899	15628	38117	30	20260	49415	38.9
Car #6	101662	15903	38788	30.5	20616	50283	39.6
Car #7	103436	16181	39466	30.8	20976	51161	40
Car #8	105199	16457	40139	31.6	21334	52034	41
Car #9	106950	16731	40807	32.4	21689	52900	42
Car #10	108713	17006	41478	32.7	22046	53771	42.3
Note	<ol style="list-style-type: none"> Coupler angle takes 1.26° for aligned position and 9° for jack-knifed position Tank cars: length 713 inches, truck center distance 550 inches Locomotive: length 826 inches, truck center distance 522 inches 						

5.4 Transformed Lateral Forces from In-train Force

5.4.1 The transformed lateral force from the in-train force depends on the positions of the couplers and car-body. If the train was in theoretical alignment, all the couplers and car bodies would be in aligned position, the coupler angles would be the minimum and the transformed lateral force would be the minimum. However, as recent studies (Ref 3, 4) and investigation experiences showed that, under coupler jackknifing condition, the coupler angle could reach its maximum limit under the buff force due to the positive feedback mechanism, and in-train buff

- force can be transformed into significant lateral force and contribute to derailment.
- 5.4.2 There could be four different combinations of coupler and car-body positions: a) both coupler and car-body in alignment position, b) coupler in alignment but car-body in jackknifed position, c) coupler in jack-knifed position but car-body in alignment position, and d) both coupler and car-body in jack-knifed position. Scenario a) generates the minimum coupler angle and transformed lateral force, and scenario d) generates the maximum coupler angle and transformed lateral force.
- 5.4.3 On the derailment curve of 4.25° , the equal length of the tank cars, 59 feet 5 inches, would cover a circle angle of approximately 2.52° . If the couplers were in alignment position, the coupler angle would be half of the circle angle, i.e. 1.26° . If the couplers were in a jack-knifed position under buff in-train force, the positive feed-back mechanism could push the coupler angle to the maximum angle. For the E type couplers on the tank cars, the maximum coupler angle would be 9° .
- 5.4.4 If the car-body was in aligned position, the transformed lateral force at each truck center would be equal to that at the coupler. But if the car was in a jack-knifed position, the transformed lateral force at the truck center would be amplified by a ratio of the car length over the truck center distance. The transformed lateral forces at truck center L_{tr} and the unloading ΔV on the inner rail under the four position scenarios are calculated and also listed in Table 5.
- 5.4.5 The transformed lateral forces acted at the coupler height above the rail top, different from the centrifugal force that acted at the center of gravity. The transformed lateral force also induced a vertical load shift that led to an unloading on one side while overloading on the other rail. The unloading percentages from the in-train force alone were far below the safety limit.
- 5.5 Combination of Centrifugal Force and In-train Force
- 5.5.1 The runaway train was subjected to the combination of the centrifugal force and the in-train buff force at the derailment moment. The resulting combined lateral forces and unloading are calculated and listed in Table 6.
- 5.5.2 The combined lateral force and unloading closely depend on the coupler and car-body positions. If no coupler was jack-knifed, the coupler angle would be very small on the curve (approximate 1.26 degrees). The transformed lateral force would be minor. The combined lateral force and unloading would still be in the relatively safe range. Therefore the additional dynamic force generated from the track geometry would be the necessary to cause the derailment.
- 5.5.3 If any coupler went into jack-knifed position under the buff in-train force in Position c and d as per paragraph 5.4.2, the combination of the centrifugal force and in-train force would induce extremely high lateral forces that exceed the track resistance and the inner wheels could be lifted. The cars could derail no matter if the car-body was in aligned or jack-knifed position, as in both positions extremely high lateral forces at the outer (high) rail and unloading at the inner (low) could

be generated. Comparatively the jack-knifed car-body position produced higher transformed lateral forces than the aligned car-body position. Under such high lateral forces and unloading percentage, the possible derailment scenarios could be in the form of widening gauge, breaking/deflecting high rail, wheel lift from the low rail and possibly striking the switch point rail.

Table 6: Combined Lateral Forces and Unloading

Parameters\Vehicle	Tank Car A	Tank Car B	Locomotive	Comment	
ΔV_a	lb	5168	5832	4666	Position a: aligned coupler and aligned carbody
ΔV_{1a}	lb	88522	91251	107627	
$\Delta V_{1a}/V_0$	%	69	71	55	
V_{min1a}	lb	39478	36749	87373	
L_{tra}	lb	2119	2391	1913	
L_{tsa}	lb	1060	1196	957	
L_{ts1a}	lb	18465	18926	23688	
ΔV_b	lb	6700	7561	7383	Position b: aligned coupler and jack-knifed carbody
ΔV_{1b}	lb	90054	92980	110344	
$\Delta V_{1b}/V_0$	%	70	73	57	
V_{min1b}	lb	37946	35020	17656	
L_{trb}	lb	2747	3100	3027	
L_{tsb}	lb	1374	1550	1514	
L_{ts1b}	lb	18779	19280	24245	
ΔV_c	lb	36771	41478	33188	Position c: jack-knifed coupler and aligned carbody, wheel lift risk on tank cars
ΔV_{1c}	lb	120125	126897	136149	
$\Delta V_{1c}/V_0$	%	94	99	70	
V_{min1c}	lb	7875	1103	7875	
L_{trc}	lb	15076	17006	13607	
L_{tsc}	lb	12595	16659	6804	
L_{ts1c}	lb	30000	34389	29535	
ΔV_d	lb	47668	53771	52515	Position d: jack-knifed coupler and jack-knifed carbody, wheel lift on all vehicles
ΔV_{1d}	lb	131022	139190	155476	
$\Delta V_{1d}/V_0$	%	100	100	100	
V_{min1d}	lb	-3022	-11190	-27476	
L_{trd}	lb	19544	22046	21531	
L_{tsd}	lb	19544	22046	21531	
L_{ts1d}	lb	36949	39776	44262	
Note	Negative values for V_{min1d} indicated wheel lift for the vehicles. Subscript 1 for centrifugal force, a-d for in-train force at positions.				

5.6 Vampire Simulation Results

5.6.1 The first derailed cars were traveling at 65 mph, much higher than the balance speed of the curve at the superelevation and the speed limit of the section. The cars were inclined to the high rail. The in-train buff force also pushed the cars toward the outside of the curve. The track geometry irregularities generated bouncing and rocking. The most critical derailment related indicators were lateral force and wheel L/V ratios on the high rail, and the unloading on the low (inside) rail. According to AAR Chapter XI, the limit of wheel L/V ratio is 1.0, and the

limit of unloading is 90% (or 10% vertical load relative to static load is left). The industry experience takes 20 kips as the risk threshold of the wheel lateral force against the track strength. The truck side L/V and axle sum L/V ratio are the indicators of a similar nature to evaluate the risk of rail rollover and track breaking through. In the following analysis, the discussions focus on the wheel lateral force and wheel L/V ratios on the high rail, and the unloading on the low (inside) rail.

- 5.6.2 It must be noted that the Vampire vehicle track dynamic simulations were performed on a generalized car model with nominal wheel/ rail profiles, which are sensitive to the results, and the track geometry data was recorded 11 months before the occurrence. The simulation results were qualitative references for estimating the effects of the contribution factors rather than an accurate quantitative reflection of the state on the day of the occurrence. However, these qualitative references were helpful in demonstrating the relative contributions and roles of the three factors in the derailment.
- 5.6.3 The output derailment indicators around the POD are plotted in Figures 14 to 28 and the statistic results of the 40 foot section centered by the POD are summarized and listed in Table 7. More detailed data are attached in Appendix C. Reported results were filtered with a 15 Hz 4 pole low pass filter. Vampire uses the dynamic loading percentage V/V_0 as the unloading index.

Table 7: Simulated Derailment Indicators around the POD

Case	Condition	Wheel L/V		Loading V/V_0 (%)		Lateral Force L (lb)	
		mean	max	mean	min	mean	max
1	MeasuredTrack_9DegF100V65	0.44	0.74	14.9	-1.8	23,163	47,965
2	MeasuredTrack_1p26DegF100V65	0.33	0.51	6.7	-0.5	17,464	36,081
3	MeasuredTrack_NoForceV65	0.31	0.45	8.6	-0.9	15,862	29,871
4	MeasuredTrack_9DegF100V30	0.23	0.34	63.6	55.2	9,735	15,345
5	IdealCurve_9DegF100V65	0.39	0.40	4.8	-0.0	23,769	24,541
6	IdealCurve_1p26DegF100V65	0.28	0.31	19.0	9.8	15,537	17,662
7	IdealCurve_NoForceV65	0.25	0.29	27.0	16.8	13,505	16,602
8	TrackGeomOnly_NoCurve_NoFV65	0.25	0.39	78.0	21.6	5,672	12,610
Note	<ol style="list-style-type: none"> 1. V_0 is the static load. 2. The maximum wheel L/V and lateral force are on the high rail 3. The minimum loading (max unloading) is on the low (inside) rail, negative value means wheel lift 4. Derailment thresholds: wheel L/V 1.0, V/V_0 10%, L 20,000 lbs 						

- 5.6.4 The mean and max/min values in the ideal curve cases are relatively close to each other respectively, indicating the nature of ideal track geometry that produces small oscillations, as in Figures 22 to 25 (including some effect of the theoretical transition from spiral to curve on the unloading approaching the POD). The measured track geometry produced significant dynamic response, being reflected by the large differences between the mean and the max/min values and shown in the plotted figures. The left wheel L/V ratios in all the cases were below the derailment criterion as the lateral force increased simultaneously as the vertical force did on the high rail from the centrifugal force and in-train force. The derailment unlikely occurred in the form of wheel climbing.

- 5.6.5 Case 7 on ideal curve with no in-train force at speed 65 mph is the dynamic simulation of the centrifugal force on the ideal curve of 4.25 degrees. Compared with the steady state calculated results in Table 4, the simulated dynamic lateral force, wheel/L/V ratio and unloading percentage are higher than the steady state calculated results showing the dynamic vibration of the vehicle on even ideal track geometry. All those indicators are below the derailment thresholds, indicating that the centrifugal force alone is not sufficient to roll over the car.
- 5.6.6 Case 5 and 6 shows the effect of the coupler angle in the combination scenarios of centrifugal force and in-train force. If the couplers were aligned (Case 6, at the minimum angle of 1.26 degrees, equivalent to scenario a in Table 6), the contribution of the in-train force would be minor. If the couplers were jack-knifed to the maximum angle of 9 degrees, the in-train force would significantly contribute to the derailment indicators. The maximum lateral force would exceed the threshold while the loading percentage would reach the criterion (Case 5, equivalent to the position c scenario in Table 6). It is interesting that the simulated unloading around the POD in dynamic Case 5 is very close to the steady state one in Table 6. However, the simulated dynamic lateral force around the POD is much higher than the steady state calculated results. The simulation Case 5 and 6 confirmed that the combination of the centrifugal force and the in-train force might be safe if the couplers and the cars were aligned, but could impose severe derailment risk if the couplers were jackknifed.
- 5.6.7 All Case 1, 2, 3 and 5 generated negative loading percentages, which indicated complete wheel lift, and excessive lateral forces. The actual derailment scenario must be between Case 1 and 2 with the combination of the three contribution factors. Case 3 shows that even without the contribution of in-train force, the combination of the centrifugal force and the dynamic bouncing/rocking generated by the track geometry at the high speed could be sufficient to cause derailment.
- 5.6.8 Case 4 clearly shows the critical effect of the speed. If the speed were 30 mph, the contribution from the three factors together would produce the derailment indicators well below the derailment thresholds, and no derailment would occur.
- 5.6.9 Case 8 demonstrates the contribution from the track geometry irregularities solely. All the simulated derailment indicators in Case 8 are below the derailment thresholds, indicating that the track geometry irregularities alone would not be sufficient to derail the cars even at the high speed of 65 mph.
- 5.6.10 Comprehensive analysis of the combinations of the three factors determined that the derailment was caused by the combination of the centrifugal force, the dynamic bouncing/rocking generated by the track geometry irregularities and the in-train force. The derailment was inevitable due to the high speed of 65 mph.
- 5.6.11 Any one of the following factors, centrifugal force, the track geometry irregularities or the in-train force would not be sufficient to cause the derailment.
- 5.6.12 The centrifugal force due to the high speed at the curve contributed most to the derailment, while the track geometry irregularities and the in-train force were the secondary contributors.

5.6.13 The contribution of the in-train force depends on the positions of the couplers and the cars. If the couplers and cars were aligned, the contribution of the in-train force would be minor. If the couplers were jack-knifed to the maximum angle, the contribution of the in-train force could be significant. The combination of the centrifugal force and the in-train force under coupler jack-knifed position could impose severe derailment risk.

6.0 CONCLUSIONS

- 6.1 The derailment was caused by the combination of the centrifugal force, the dynamic force generated by the track geometry conditions and the in-train buff force. In consideration of these factors, the derailment was inevitable due to the high speed of 65 mph.
- 6.2 Any one of the following factors, centrifugal force, track geometry irregularities or in-train forces, would not be sufficient to cause the derailment.
- 6.3 The centrifugal force due to the high speed at the curve contributed most to the derailment, while track geometry irregularities and in-train forces were secondary contributors.
- 6.4 The rollover speeds due to the centrifugal force on the 4.25⁰ curve were calculated to be approximately 83.0 to 83.9 mph for the derailed loaded tank cars and 92.7 mph for the involved locomotives, at a superelevation of 1 ½ inches.
- 6.5 The train speed at the derailment moment was significantly below the rollover speeds of the vehicles on the curve, and the lateral forces and unloading from the centrifugal force were within the acceptable range. The centrifugal force alone would not rollover the vehicles to cause the derailment as long as the track was intact.
- 6.6 The track geometry condition at the POD on the day of occurrence could not be determined quantitatively. If the track geometry defects recurred to the levels noted in the previous inspection, they could generate significantly high dynamic forces, contributing to the derailment.
- 6.7 The track geometry irregularities alone would not be sufficient to derail the cars even at the high speed of 65 mph.
- 6.8 Combination of the centrifugal force and the dynamic forces generated by the track geometry at speed of 65 mph could be sufficient to cause derailment.
- 6.9 The speed is critical to the centrifugal force and the dynamic force generated by the track geometry. At 30 mph, the contribution from the three factors would result in derailment indicators well below the derailment thresholds.
- 6.10 The simulated in-train buff forces at the derailed tank cars were approximately 100 to 110 kips, which alone would not cause derailment of the loaded vehicles in the occurrence.
- 6.11 The transformed lateral force and unloading from the in-train force closely depend on the coupler and car-body position. The coupler angle would be small if

all couplers and car-bodies were in aligned positions. If any coupler went into jackknifed position under the buff in-train force, the coupler angle could reach the maximum limit allowed by the car's striker housing.

- 6.12 If all the couplers and car-bodies were in aligned position and the track conditions were ideal, the contribution of the in-train force would be minor, and the combination of the centrifugal force and the in-train buff force would not be sufficient to cause derailment.
- 6.13 If any of the couplers was jack-knifed to the maximum angle, the combination of the centrifugal force and the in-train force under coupler jack-knifed position could impose severe derailment risk.

7.0 REFERENCES

- [1]. William H. Hay, Railroad Engineering, John Wiley & Sons Inc; ISBN: 0471364002.
- [2]. Paul Rhine, Locomotive Engineering Guide to Fuel Conservation, Simmons-Boardman Books, Inc. 1996; ISBN: 0911382178.
- [3]. D. Chen, Derailment Risk due to Coupler Jack-knifing under Longitudinal Buff Force. *Proc. IMechE, Part F: J. Rail and Rapid Transit*, 2010, 224 (F5), 483-490. DOI 10.1243/09544097JRRT363.
- [4]. D. Chen, Contributing Factors and Applicable Criteria for Jack-Knifing Derailments, Proceedings of the 10th IHHA Conference, Vol. I, New Delhi, India, Feb. 2013. pp404-410
- [5]. TÜV Rheinland Mobility Inc. Rail Sciences Division (TRRSI), Lac-Megantic Derailment VAMPIRE Vehicle Dynamics Analysis, prepared for TSB, March 12, 2014.



Figure 1: Aerial View of Derailment Site

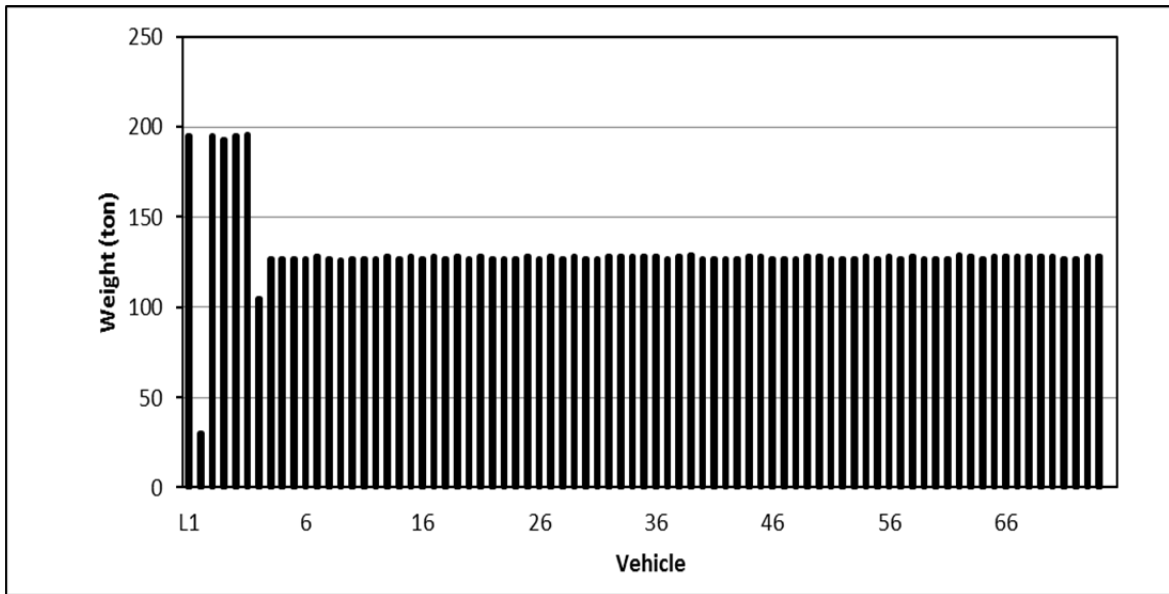


Figure 2: Train Weight Profile

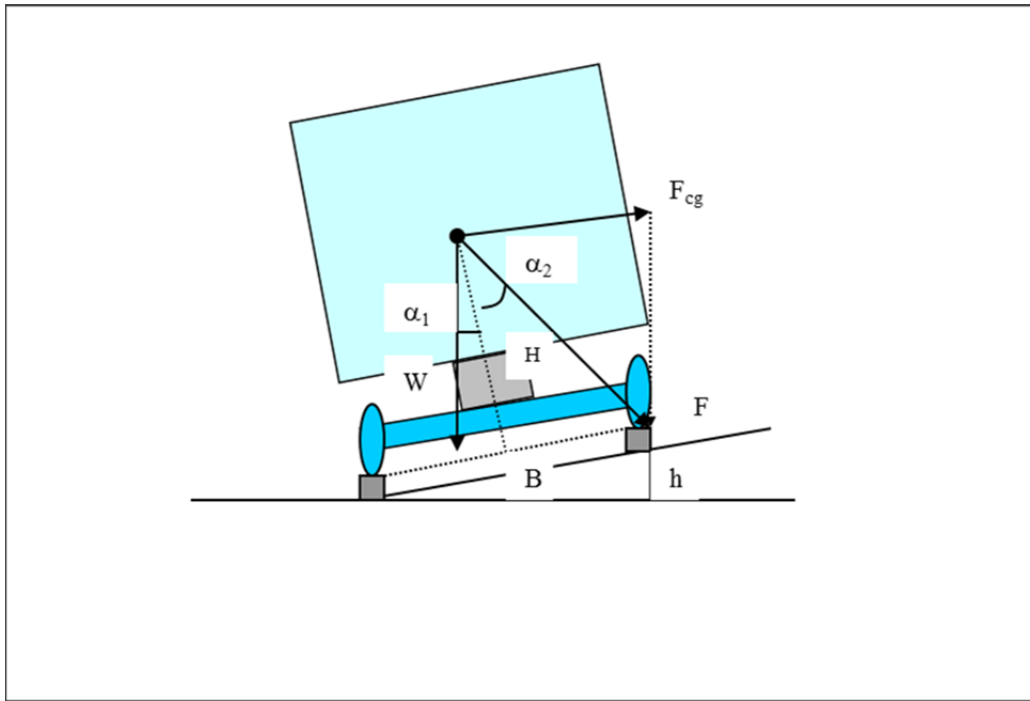


Figure 3: Centrifugal Force and Rollover Condition on Curve (diagram not to scale)

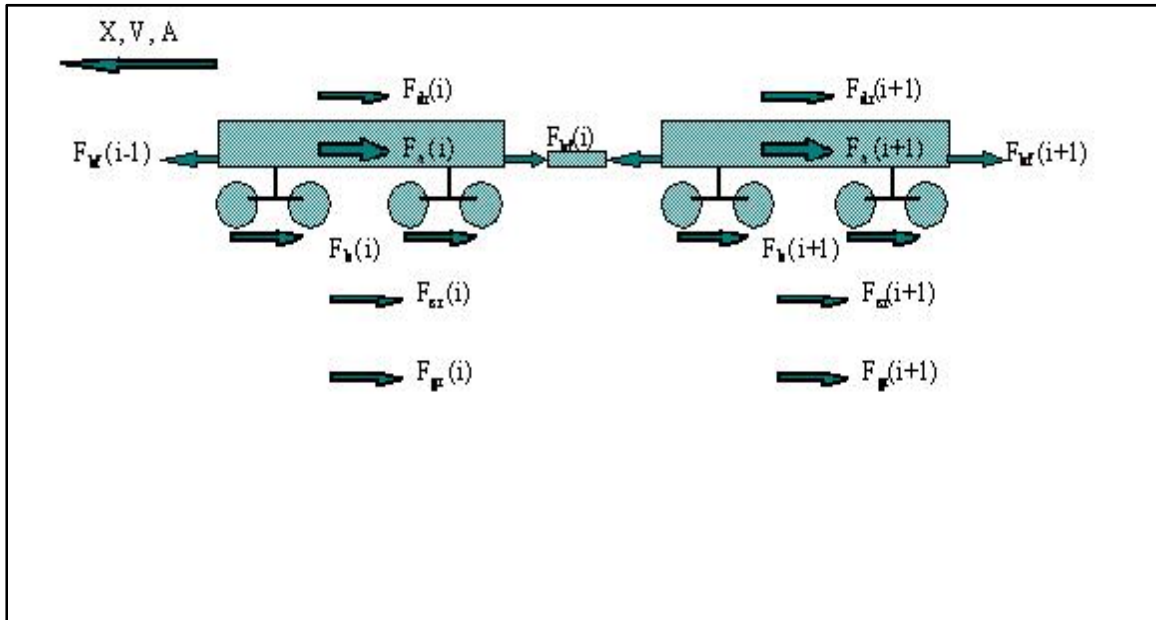


Figure 4: Longitudinal Forces on Sample Vehicle Model

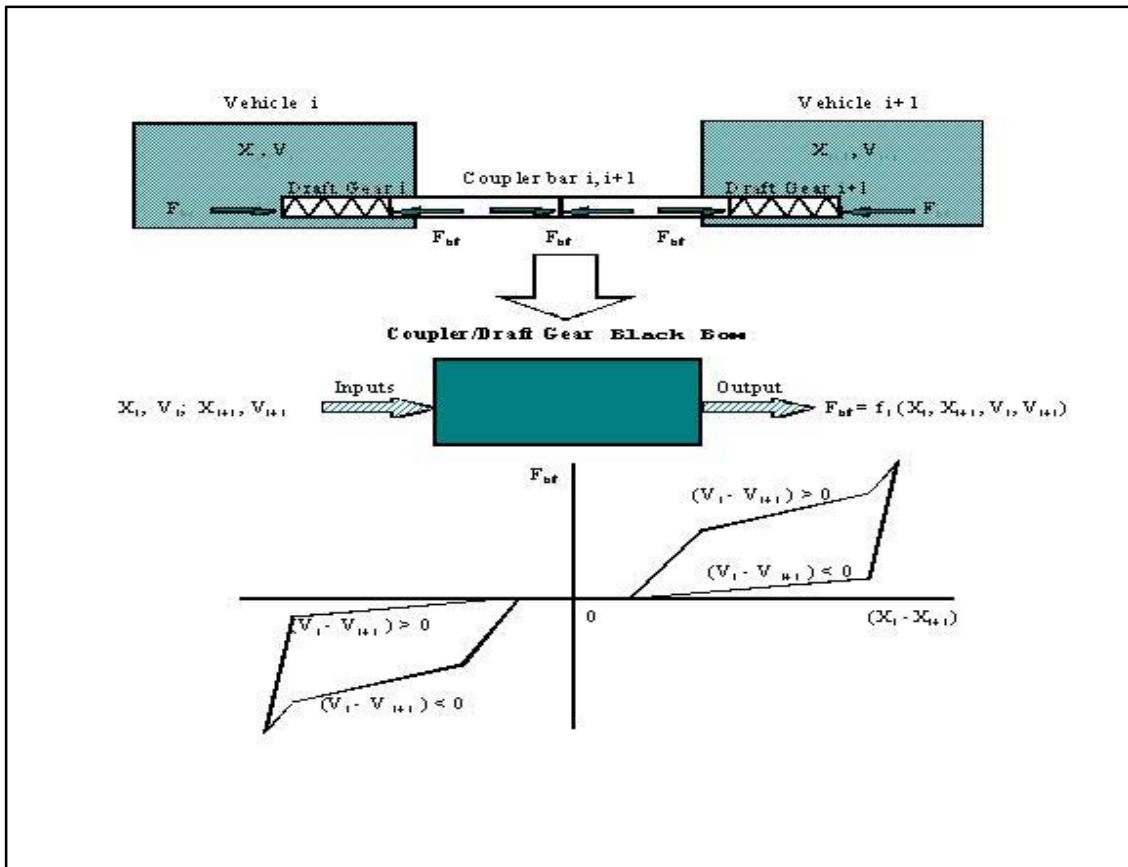


Figure 5: Coupler/Draft Gear Model

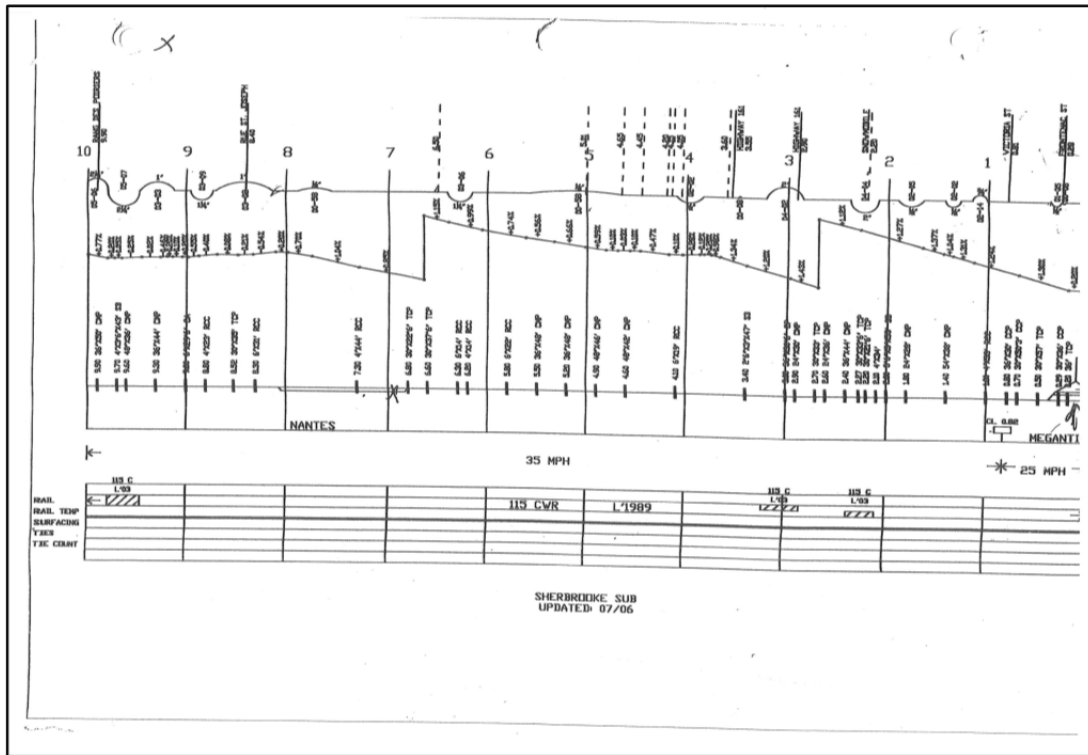


Figure 6: Grades and Curves in the Simulation Section

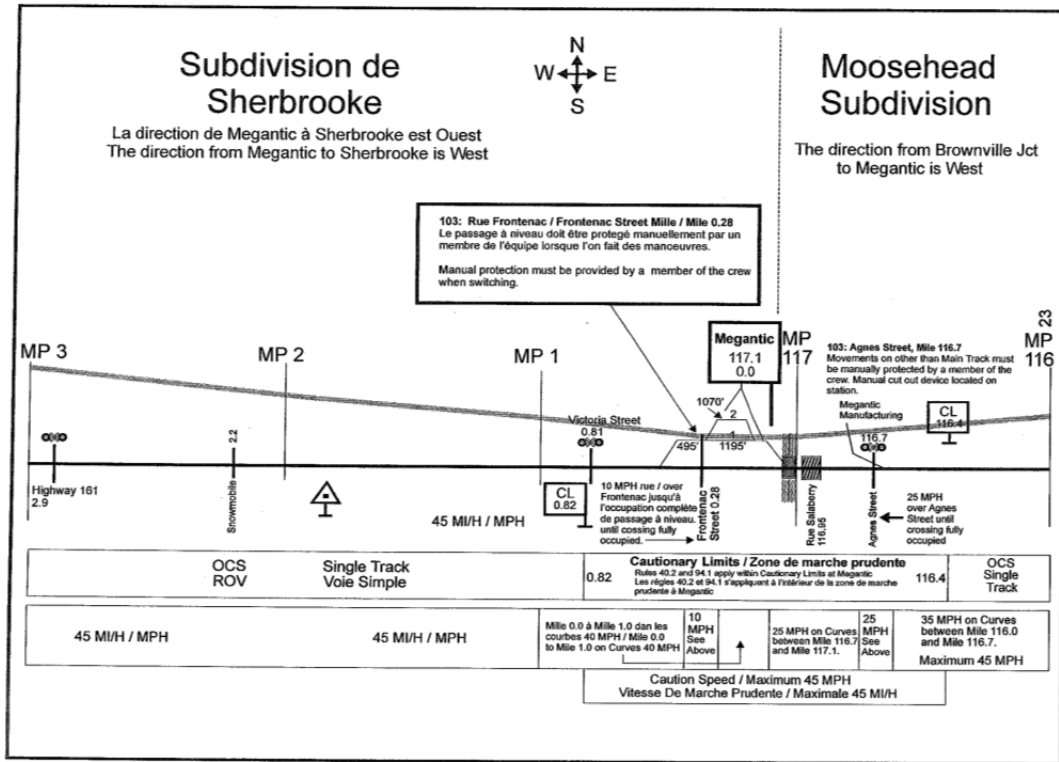


Figure 7: Grades of the Simulation Section around the POD

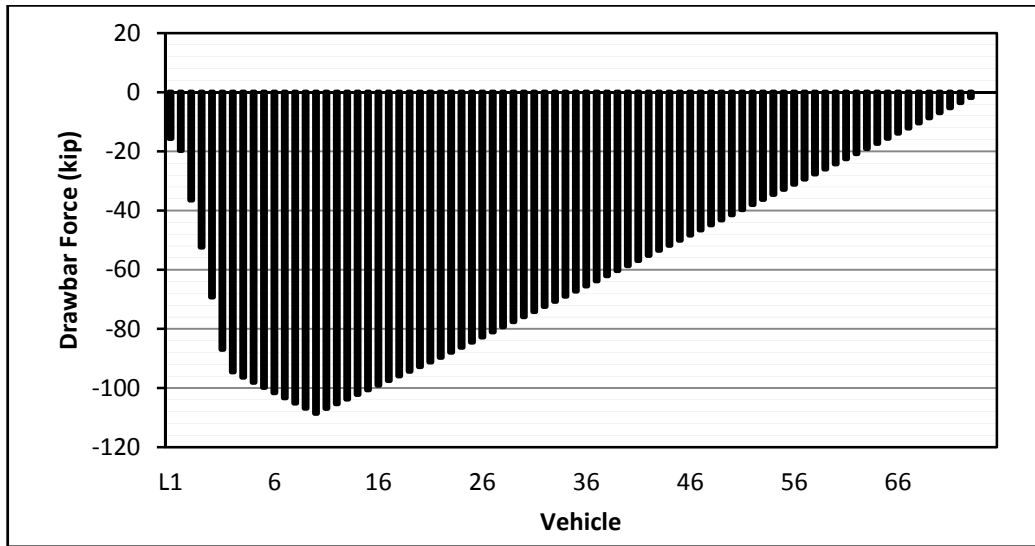


Figure 8: Simulated In-Train Force Distribution at the Derailment Moment

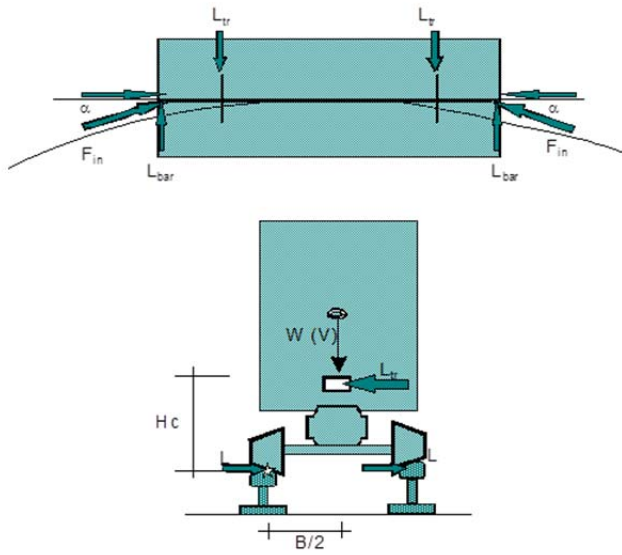


Figure 9: Schematic of Aligned Car Rollover

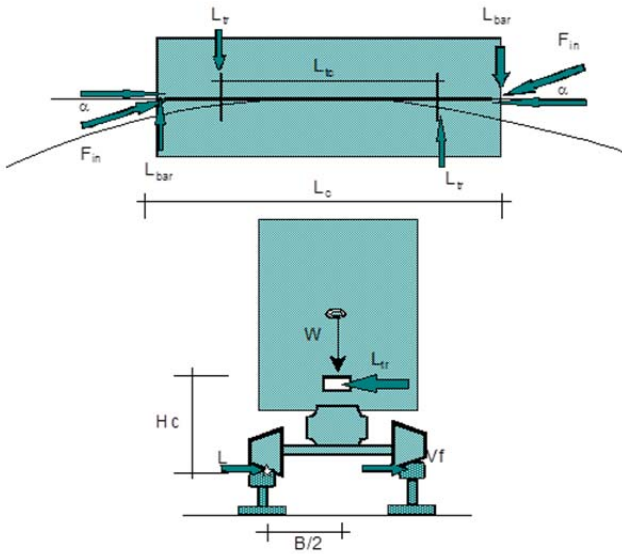


Figure 10: Forces on a Jack-knifed Car

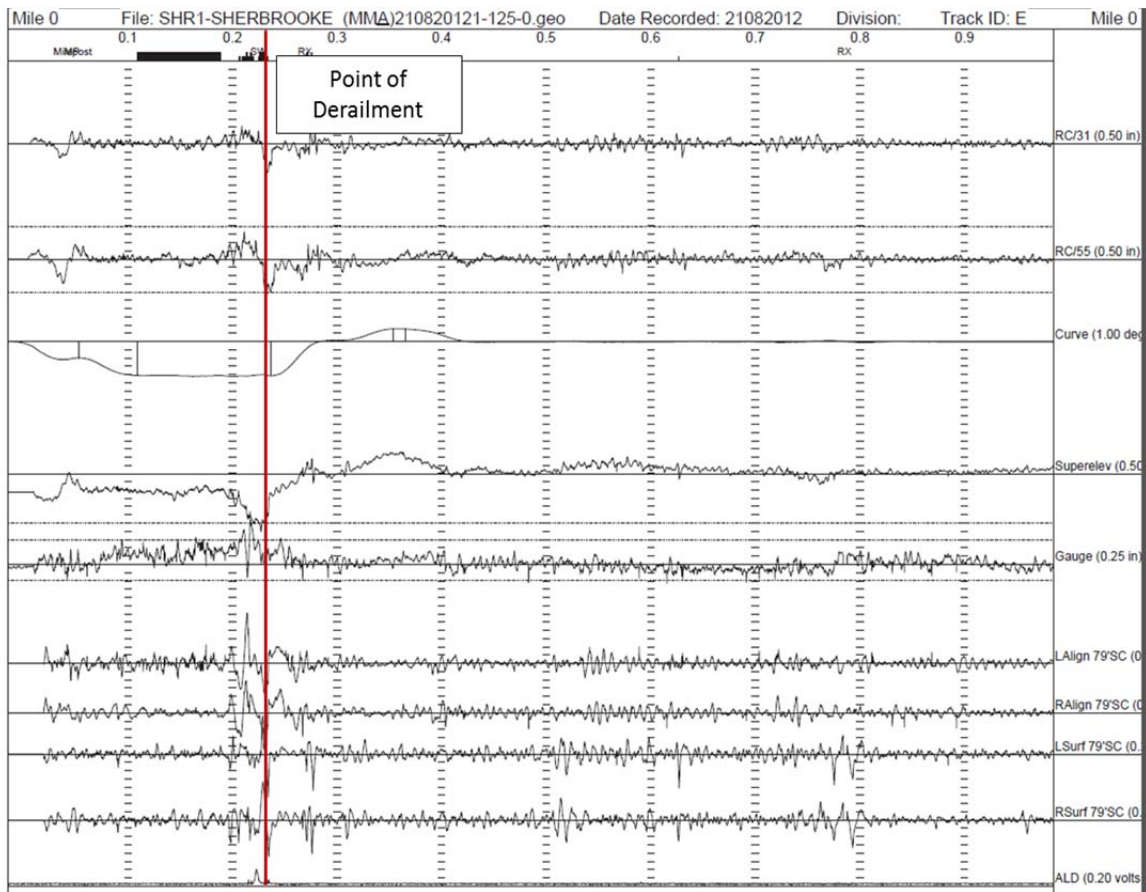


Figure 11: Track Geometry Brush Chart on 21 August 2012



Figure 12: Curve and Switch Track Section with Depressed Rail Joint Defects

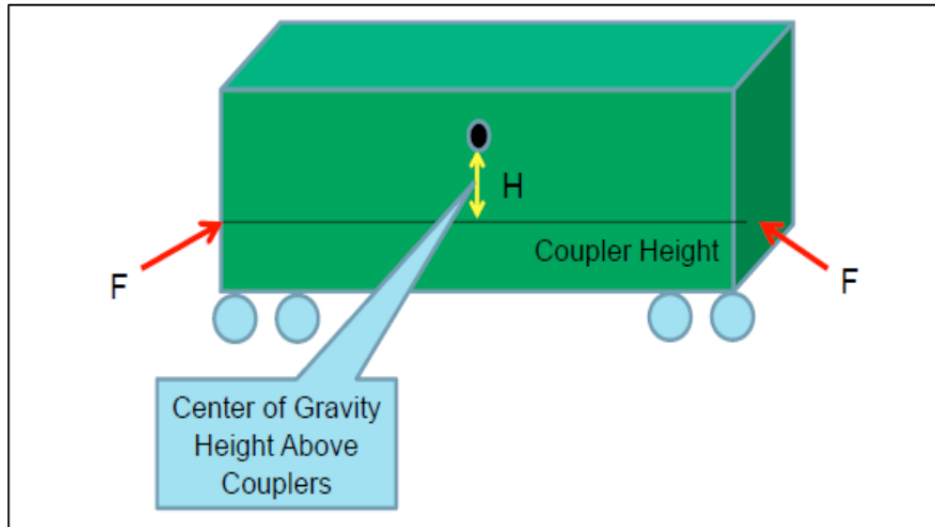


Figure 13: Breakdown of In-train Force on Vampire Vehicle Model

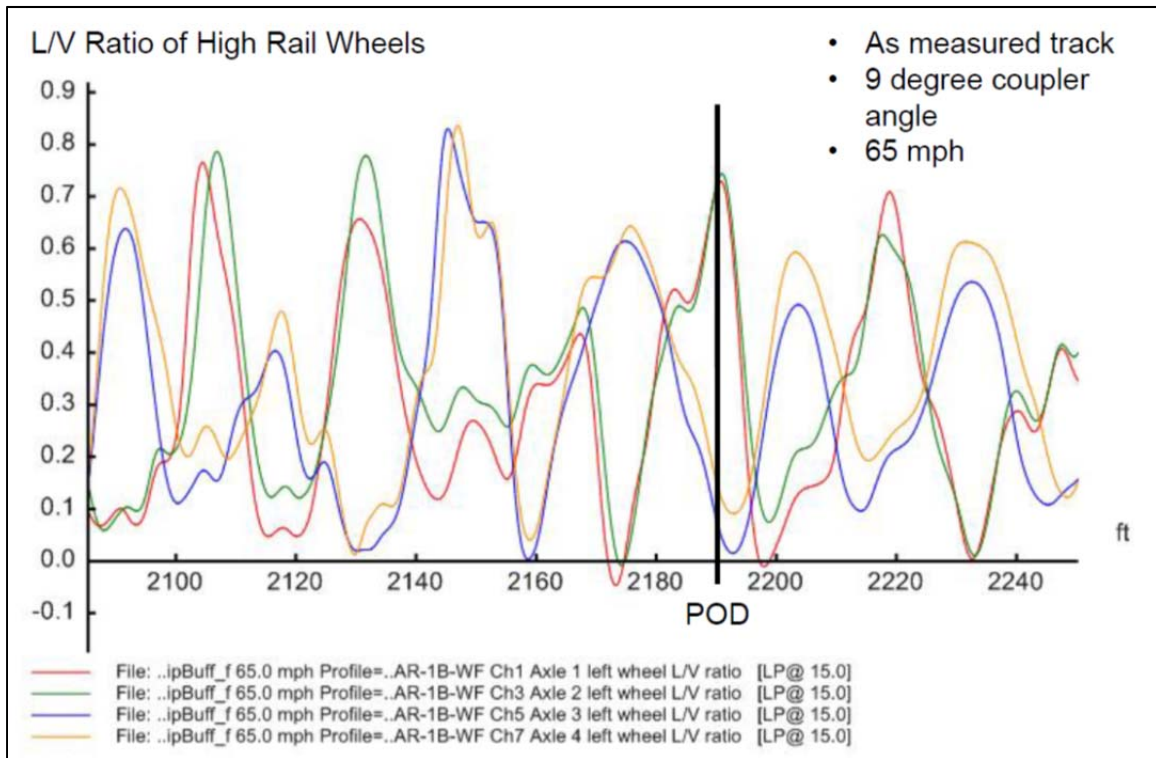


Figure 14: Wheel L/V Ratios in Case 1: MeasuredTrack_9DegF100V65

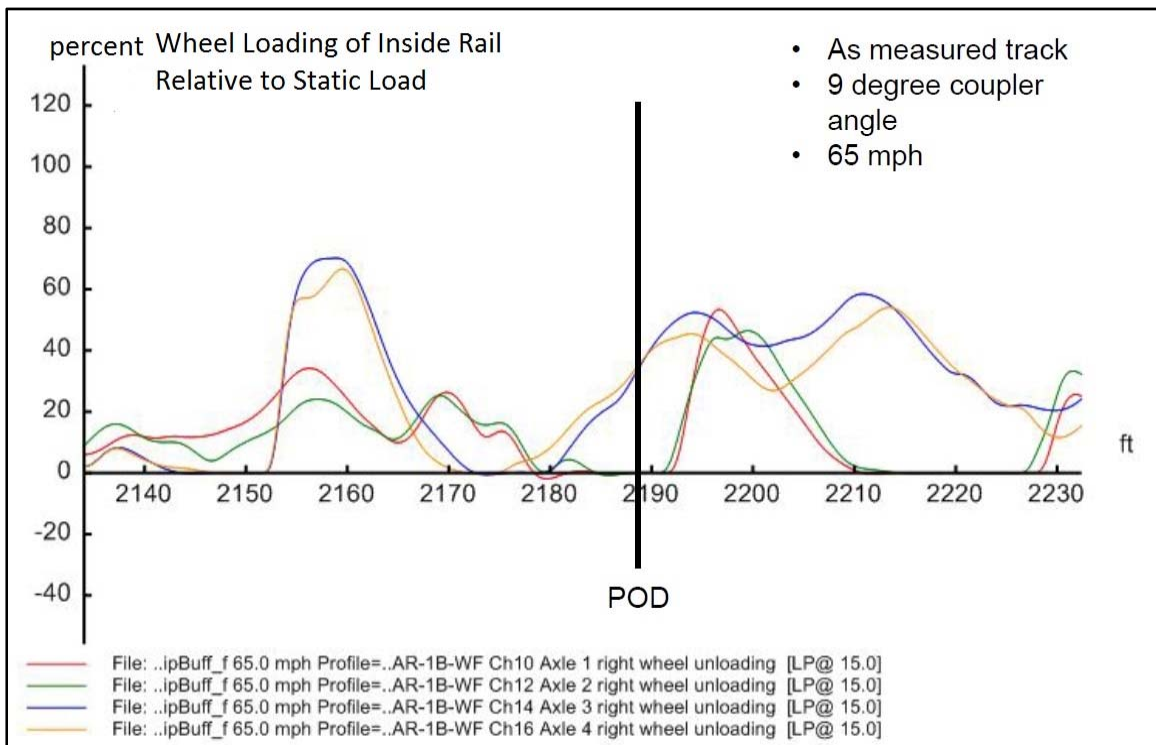


Figure 15: Wheel Loading Percentage in Case 1: MeasuredTrack_9DegF100V65

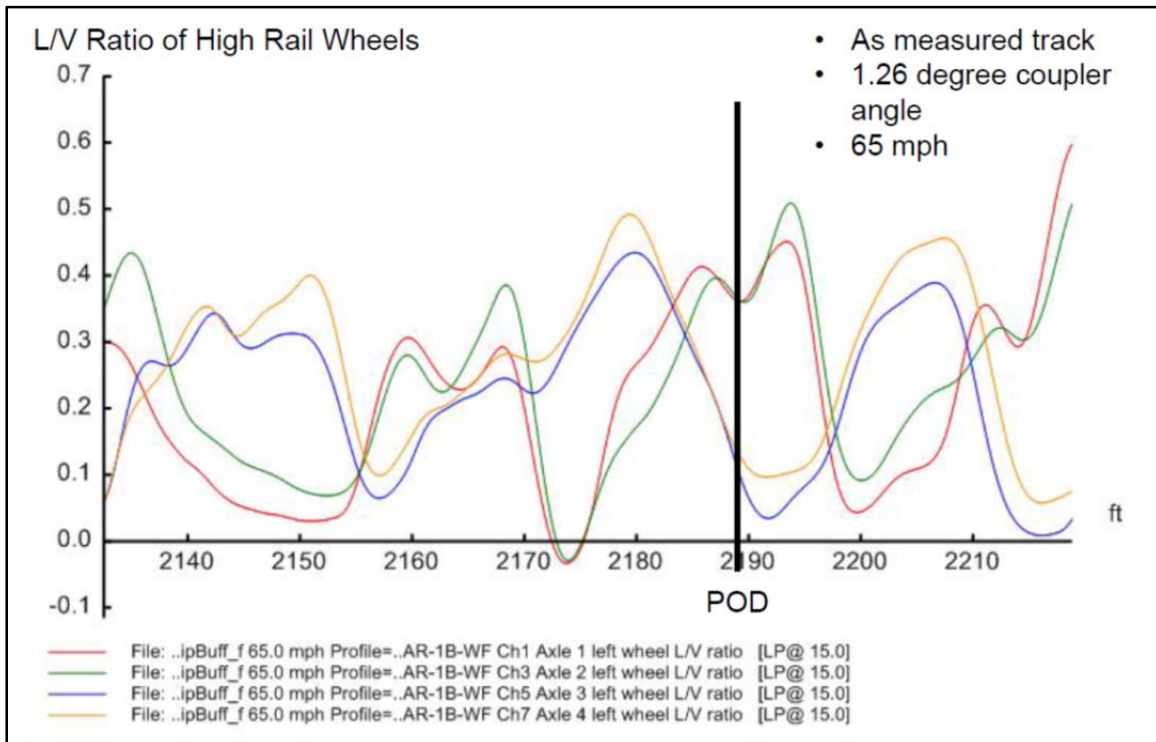


Figure 16: Wheel L/V Ratios in Case 2: MeasuredTrack_1p26DegF100V65

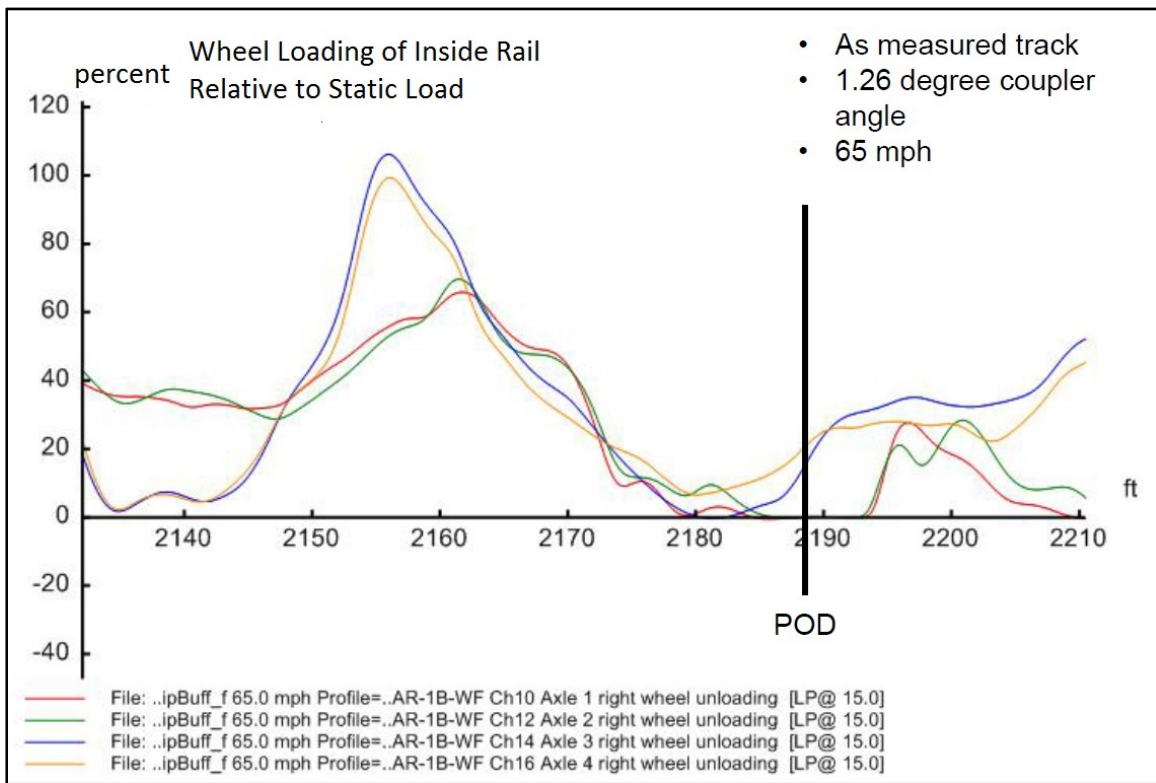


Figure 17: Wheel Loading Percentage in Case 2: MeasuredTrack_1p26DegF100V65

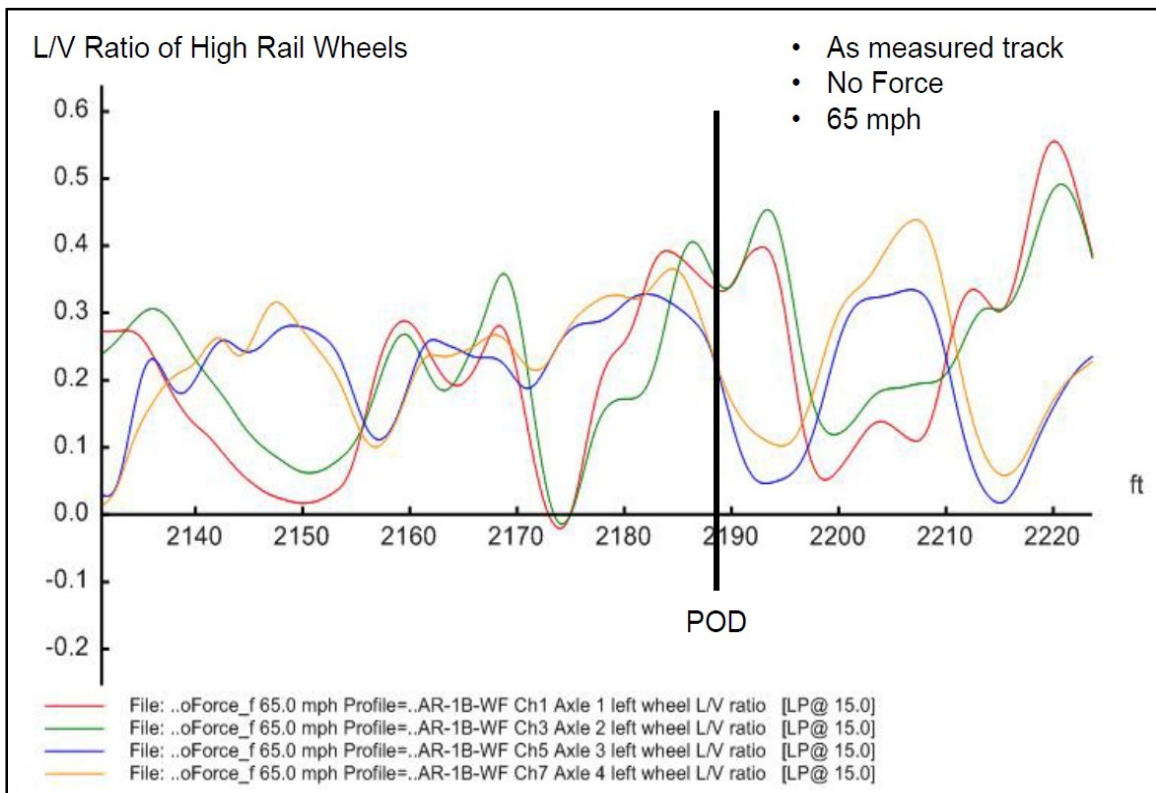


Figure 18: Wheel L/V Ratios in Case 3: MeasuredTrack_NoForceV65

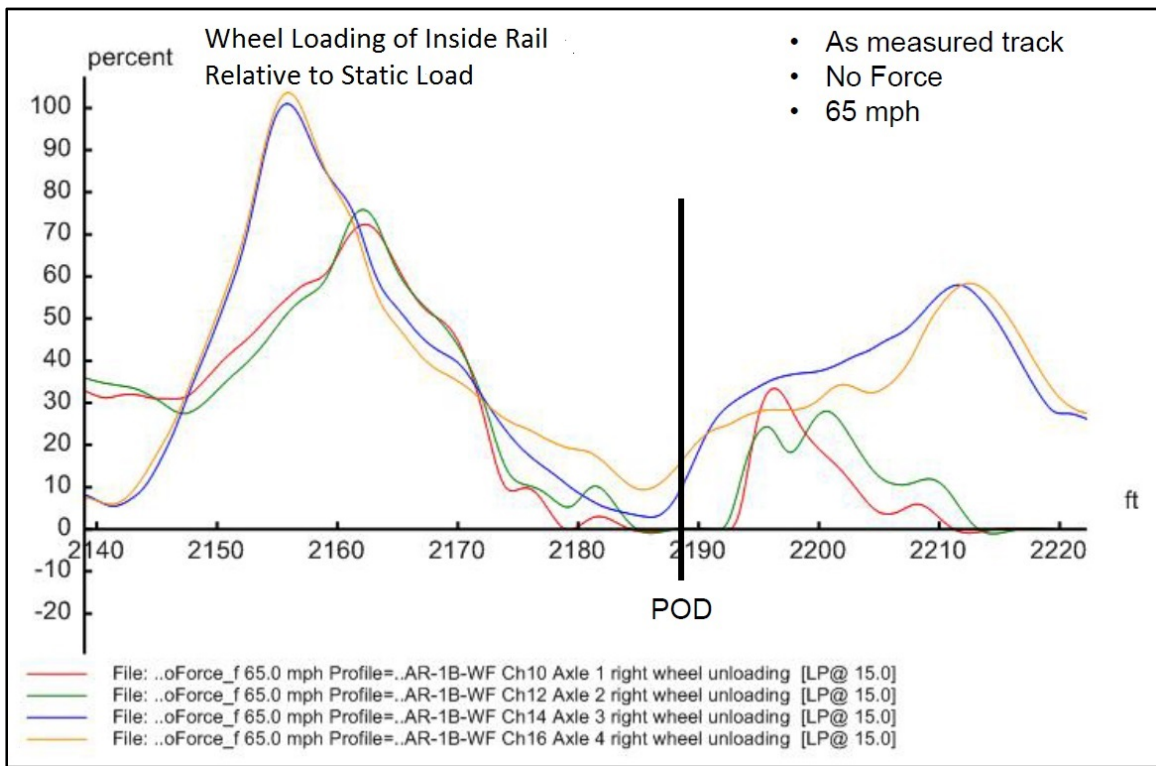


Figure 19: Wheel Loading Percentage in Case 3: MeasuredTrack_NoForceV65

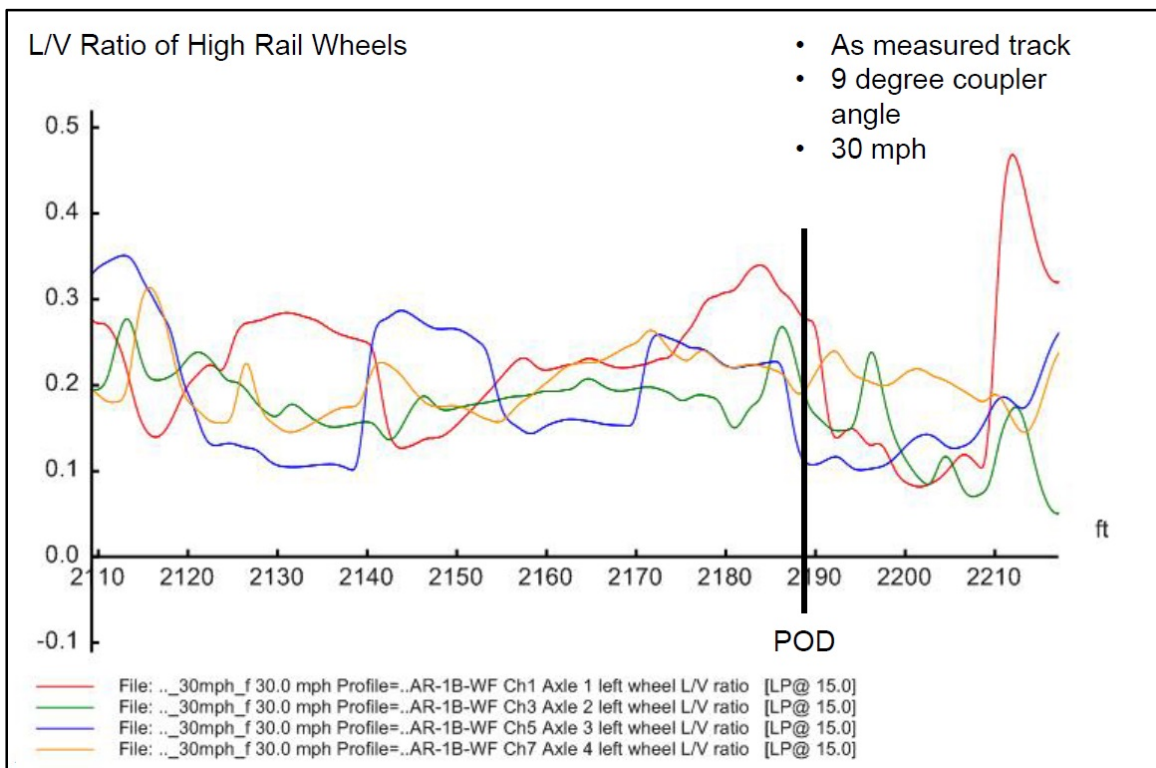


Figure 20: Wheel L/V Ratios in Case 4: MeasuredTrack_9DegF100V30

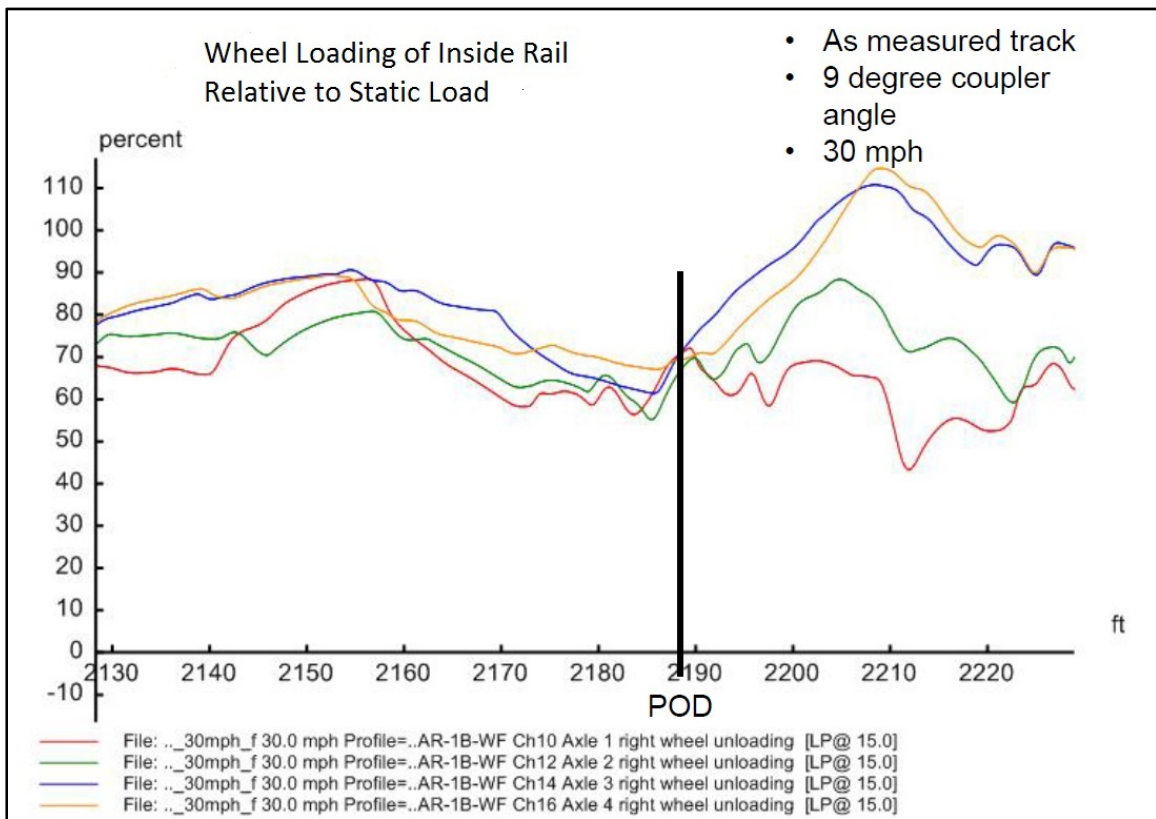


Figure 21: Wheel Loading Percentage in Case 4: MeasuredTrack_9DegF100V30

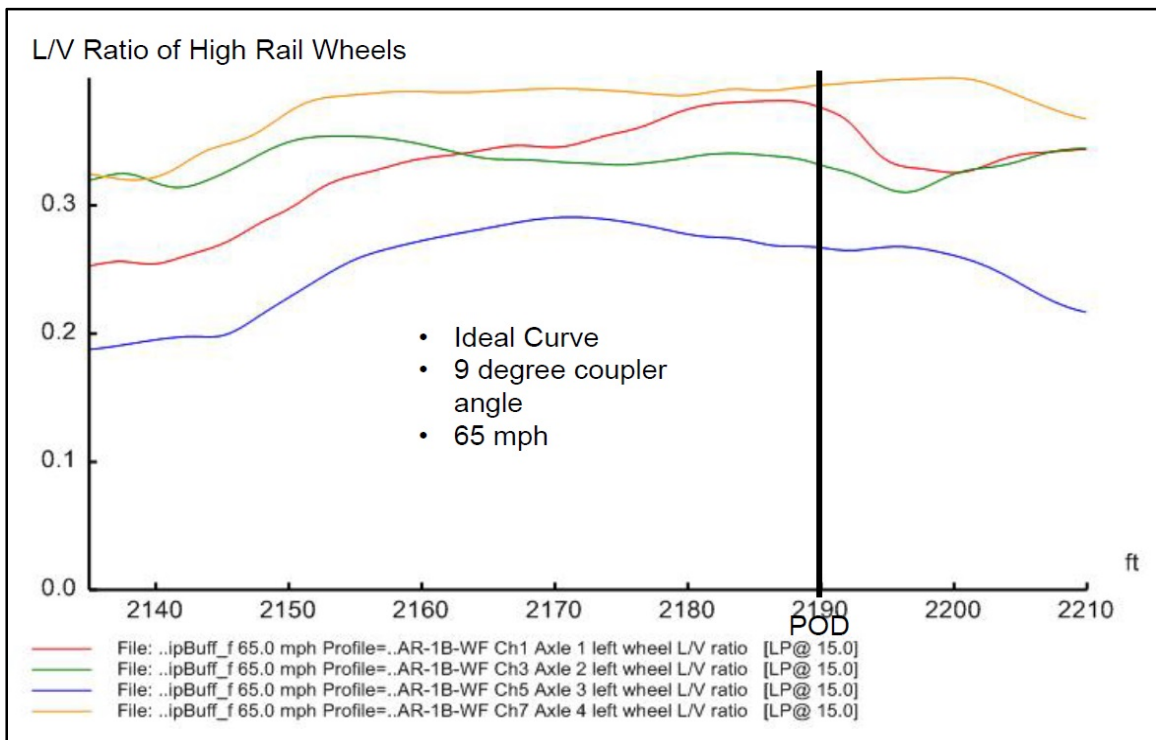


Figure 22: Wheel L/V Ratios in Case 5: IdealCurve_9DegF100V65

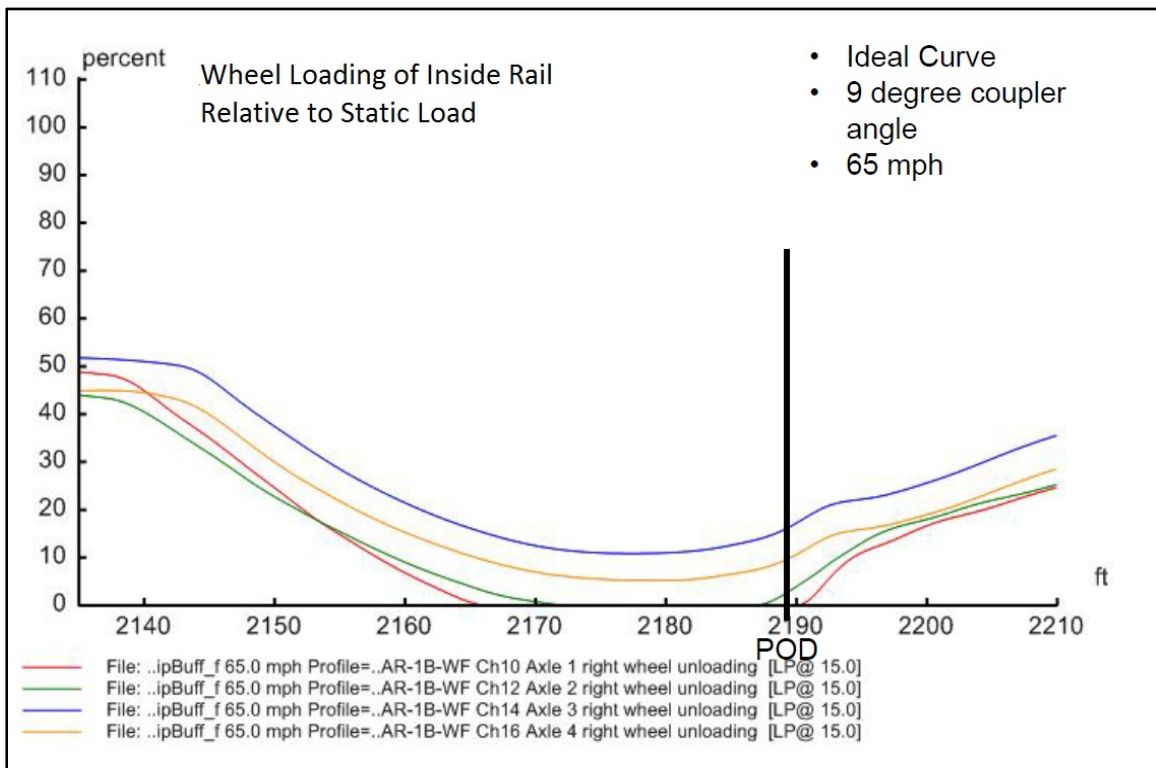


Figure 23: Wheel Loading Percentage in Case 5: IdealCurve_9DegF100V65

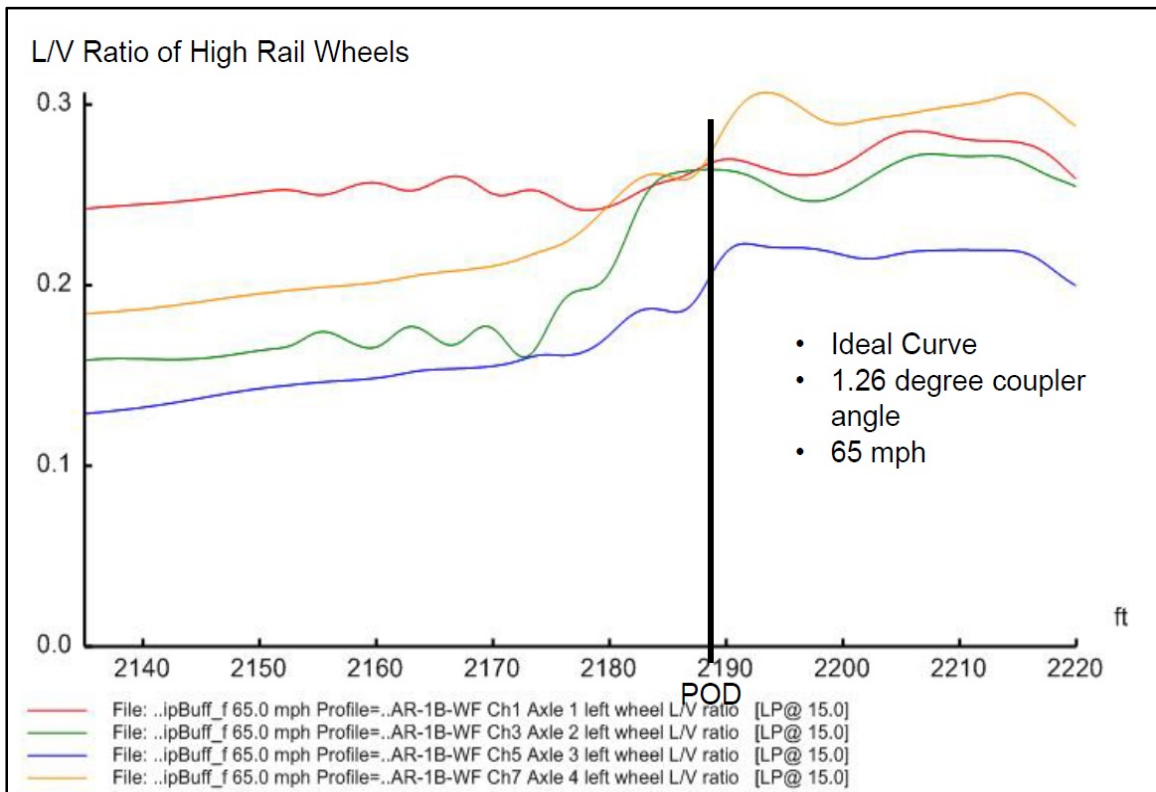


Figure 24: Wheel L/V Ratios in Case 6: IdealCurve_1p26DegF100V65

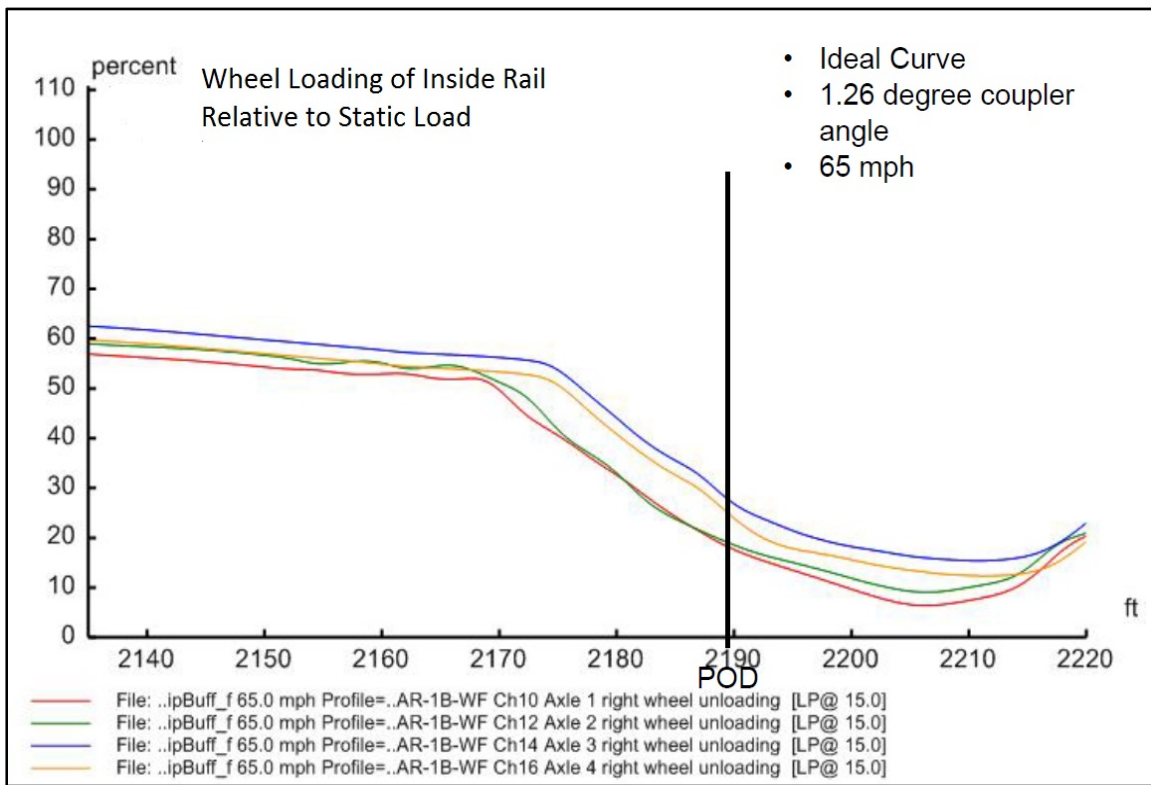


Figure 25: Wheel Loading Percentage in Case 6: IdealCurve_1p26DegF100V65

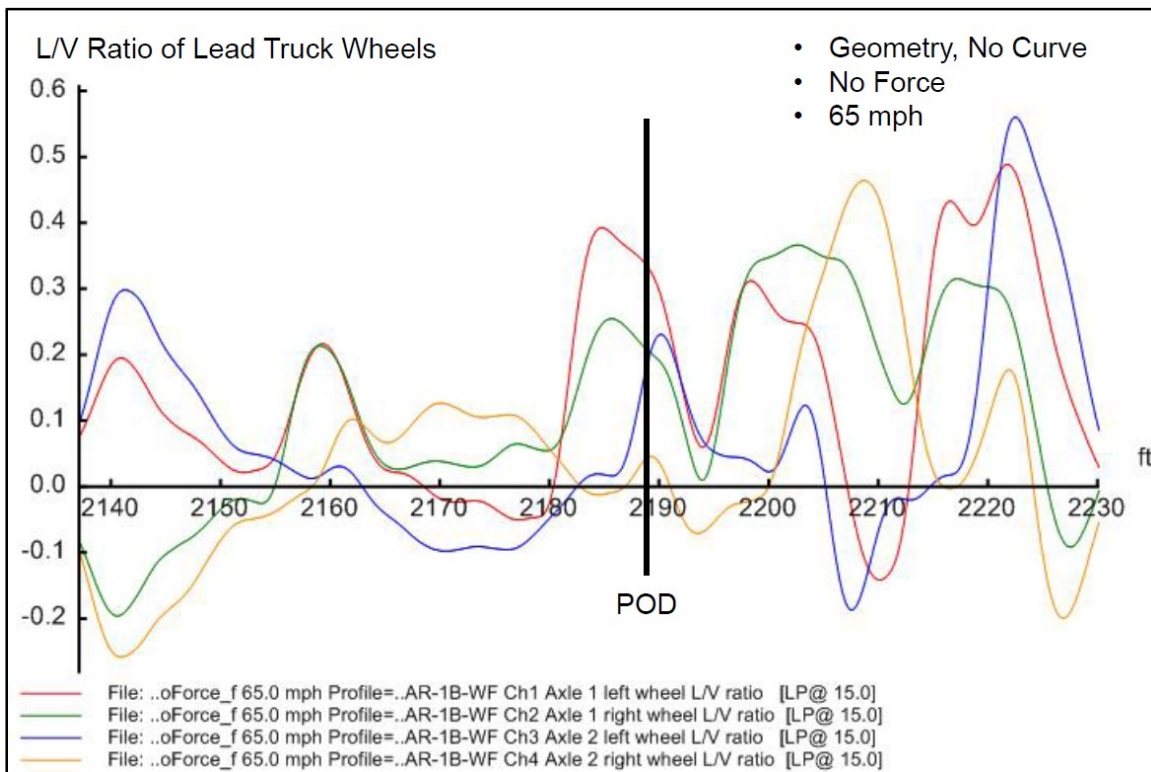


Figure 26: Wheel L/V Ratios in Case 8: TrackGeomOnly_NoCurve_NoFV65

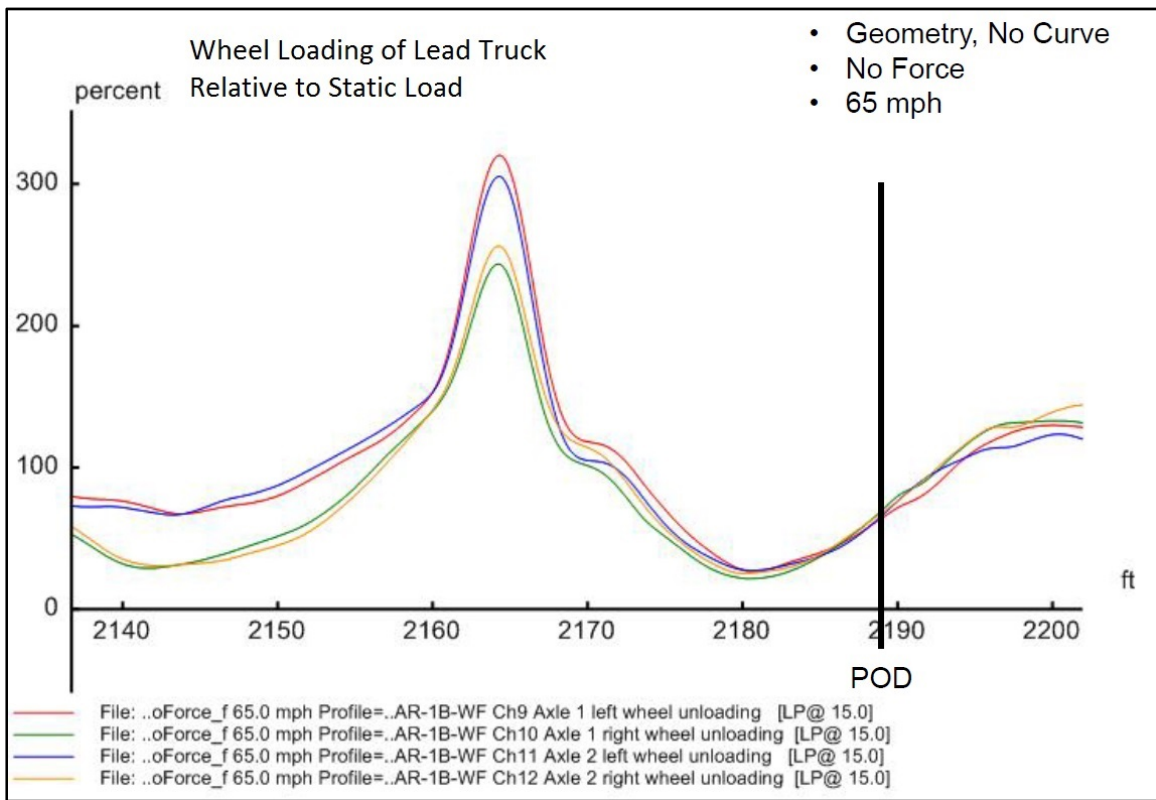


Figure 27: Wheel Loading Percentage in Case 8: TrackGeomOnly_NoCurve_NoFV65

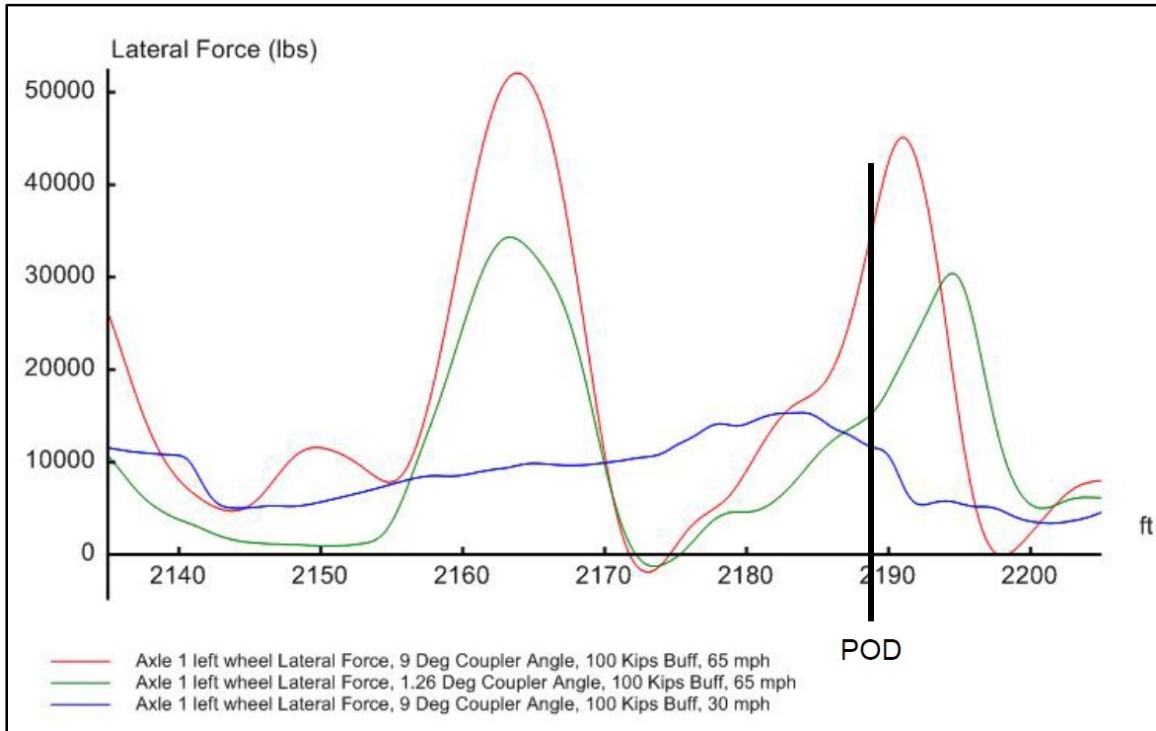


Figure 28: Sample Lateral Force of Left Lead Wheel in Case 1, 2 and 4

Appendix A: Track Geometry Defects around the POD Section

CANADIAN PACIFIC RAILWAY

TRACK EVALUATION CAR

Priority Defect Report

Date Tested: August 21, 2012

Subdivision Number: SHR1

Subdivision Name: SHERBROOKE (MM&A)

Engineering Services

DEF NO.	DEF P/U NAME	T/B C/E	FROM MLGE/FT	TO MLG/FT	LENGTH FT	MAX VAL	SPEED FRT/PAS
2396	P W GA	C	45.0 + 72	45.0 + 66	5	0 3/4"	
2397	P W GA	C	44.9 + 440	44.9 + 424	15	0 7/8"	
2398	P W GA	C	44.9 + 403	44.9 + 390	12	0 7/8"	
2399	P W GA	C	44.9 + 173	44.9 + 170	2	0 3/4"	
2400	P W GA	C	44.9 + 28	44.9 + 25	2	0 3/4"	
2401	P W GA	C	44.8 + 516	44.8 + 511	4	0 3/4"	
2402	P W GA	C	44.8 + 483	44.8 + 473	11	0 7/8"	
2403	P W GA	C	44.8 + 440	44.8 + 431	8	0 7/8"	
2404	P W GA	B	44.5 + 29	44.5 + 27	2	0 3/4"	
2405	P W GA	B	43.5 + 152	43.5 + 115	36	1 "	
2406	P W GA	B	43.5 + 90	43.5 + 81	9	0 7/8"	
2407	U AL/31	C	42.3 + 317	42.3 + 300	7	1 3/8"	25 30
2408	P*AL/31	C	42.3 + 318	42.3 + 255	19	1 1/4"	
2409	P W GA	C	41.8 + 161	41.8 + 158	3	0 3/4"	
2410	P W GA	C	41.8 + 16	41.8 + 8	7	0 7/8"	
2411	P W GA	C	41.7 + 518	41.7 + 507	10	0 7/8"	
2412	P W GA	C	41.7 + 382	41.7 + 379	3	0 3/4"	
2413	P W GA	C	41.7 + 305	41.7 + 296	10	0 3/4"	
2414	P W GA	C	41.7 + 179	41.7 + 171	7	0 3/4"	
2415	P*W GA	C	41.6 + 238	41.6 + 212	24	1 1/8"	
2416	P RC/20	C	41.6 + 206	41.6 + 201	5	1 1/8"	
2417	P R31 NR	C	41.6 + 190	41.6 + 184	7	1 5/8"	
2418	P W GA	C	41.6 + 198	41.6 + 187	6	0 7/8"	
2419	P W GA	C	41.6 + 161	41.6 + 155	7	0 7/8"	
2420	P W GA	C	40.7 + 373	40.7 + 370	2	0 3/4"	
2421	P*SPXLV	E	40.4 + 375	40.4 + 366	9	1 1/4"	
2422	P RC/20	E	40.4 + 350	40.4 + 349	2	1 1/8"	
2423	P*SPXLV	E	40.4 + 353	40.4 + 349	4	1 1/8"	
2424	P*SPXLV	E	40.4 + 346	40.4 + 338	7	1 1/8"	
2425	P RC/20	E	40.4 + 324	40.4 + 321	3	1 "	
2426	P SPXLV	E	40.4 + 330	40.4 + 321	8	1 1/8"	
2427	P*SPXLV	B	40.4 + 20	40.4 + 0	20	1 1/8"	
2428	P W GA	T	39.3 + 442	39.3 + 425	16	1 "	
2429	P*SPXLV	E	38.3 + 272	38.3 + 269	3	1 1/4"	
2430	P RC/20	E	38.3 + 272	38.3 + 257	15	1 3/8"	
2431	P*SPXLV	E	38.3 + 255	38.3 + 247	8	1 1/4"	
2432	Not Valid						
2433	P*AL/31	E	38.2 + 333	38.2 + 328	5	1 1/4"	
2434	P*W GA	E	38.2 + 334	38.2 + 322	12	1 1/8"	
2435	P RC/GA	E	38.2 + 322	38.2 + 310	11	1 3/4"	
2436	Not Valid						
2437	P RC/GA	E	38.2 + 305	38.2 + 302	3	1 1/8"	
2438	P AL/62	E	38.2 + 333	38.2 + 310	9	1 3/4"	
2439	Not Valid						
2440	Not Valid						
2441	P RC/GA	E	38.2 + 299	38.2 + 297	2	1 1/8"	
2444	Not Valid						
2442	P RC/20	E	38.2 + 310	38.2 + 291	20	1 7/8"	

Page 52

DEF NO.	DEF P/U NAME	T/B C/E	FROM MLGE/FT	TO MLG/FT	LENGTH FT	MAX VAL	SPEED FRT/PAS
2886	U RC/55	T	3.5 + 32	3.5 + 28	5	2 "	10 15
2887	P*RC/55	T	3.5 + 28	3.5 + 21	6	2 "	
2885	P RC/62	T	3.5 + 24	3.5 + 20	5	2 "	
2888	P RC/62	T	3.5 + 13	3.5 + 7	6	2 "	
2889	U RC/62	T	3.5 + 20	3.4 + 522	19	2 1/4"	10 15
2890	P RV ELV	E	3.4 + 499	3.4 + 498	2	1 5/8"	
2891	P RC/62	E	3.4 + 499	3.4 + 498	2	1 7/8"	
2892	P RV ELV	E	3.4 + 482	3.4 + 477	5	1 3/8"	
2893	P RV ELV	E	3.4 + 451	3.4 + 443	8	1 3/4"	
2894	P RC/20	E	3.4 + 442	3.4 + 440	2	1 "	
2895	P*SPXLV	E	3.4 + 442	3.4 + 434	8	1 1/8"	
2896	P RV ELV	E	3.4 + 431	3.4 + 423	8	1 3/4"	
2897	U RV ELV	E	3.4 + 443	3.4 + 431	13	2 "	25 30
2898	P RC/20	E	3.4 + 418	3.4 + 416	2	1 "	
2899	P*SPXLV	E	3.4 + 418	3.4 + 407	11	1 1/8"	
2900	P*SPXLV	E	3.4 + 400	3.4 + 395	3	1 1/8"	
2901	P RV ELV	E	3.4 + 379	3.4 + 378	2	1 1/4"	
2902	P SPXLV	E	3.1 + 448	3.1 + 446	2	1 1/8"	
2903	P*SPXLV	E	3.1 + 430	3.1 + 422	7	1 1/4"	
2904	P*SPXLV	E	3.1 + 421	3.1 + 416	4	1 1/4"	
2905	P SPXLV	E	3.1 + 413	3.1 + 403	9	1 1/8"	
2906	U SPXLV	E	3.1 + 422	3.1 + 413	6	1 1/4"	25 30
2907	P RC/62	E	3.1 + 419	3.1 + 392	27	2 "	
2908	P W GA	B	2.8 + 422	2.8 + 409	11	0 7/8"	
2909	P RC/20	B	2.8 + 356	2.8 + 353	3	1 1/8"	
2910	P SPXLV	B	2.8 + 358	2.8 + 353	4	1 1/8"	
2911	P SPXLV	B	2.8 + 347	2.8 + 345	2	1 "	
2912	P R31 SR	B	2.8 + 342	2.8 + 340	3	1 7/8"	
2913	P RC/20	B	2.8 + 337	2.8 + 334	3	1 1/8"	
2914	P SPXLV	B	2.8 + 340	2.8 + 332	8	1 1/8"	
2915	P RC/20	B	2.8 + 332	2.8 + 319	12	1 5/8"	
2916	P*SPXLV	B	2.8 + 316	2.8 + 311	4	1 1/4"	
2917	U SPXLV	B	2.8 + 332	2.8 + 316	16	1 3/4"	10 15
2918	P W GA	E	2.3 + 84	2.3 + 81	2	0 3/4"	
2919	P W GA	E	2.3 + 42	2.3 + 39	2	0 7/8"	
2920	P W GA	C	2.2 + 210	2.2 + 197	12	1 "	
2921	P SPXLV	E	1.8 + 321	1.8 + 320	2	1 "	
2922	P S22 NR	E	1.3 + 418	1.3 + 414	3	1 1/8"	
2923	P S22 NR	E	0.2 + 402	0.2 + 400	2	1 "	
2924	P*SPXLV	E	0.2 + 399	0.2 + 397	2	1 1/4"	
2925	U SPXLV	E	0.2 + 402	0.2 + 399	3	1 1/2"	25 30
2926	P*SPXLV	E	0.2 + 384	0.2 + 380	4	1 1/4"	
2927	U SPXLV	E	0.2 + 380	0.2 + 376	4	1 3/8"	25 30

DEF NO.	DEF P/U NAME	T/B C/E	FROM MLGE/FT	TO MLG/FT	LENGTH FT	MAX VAL	SPEED FRT/PAS
2928	P W GA	E	0.2 + 244	0.2 + 241	3	0 3/4"	
2929	P RC/62	C	0.2 + 175	0.2 + 173	2	1 3/4"	
2930	P RC/62	C	0.2 + 168	0.2 + 163	5	2 "	
2931	P RC/20	C	0.2 + 181	0.2 + 162	19	1 3/8"	
2932	P R31 NR	C	0.2 + 157	0.2 + 154	3	1 7/8"	
2933	P RC/62	C	0.2 + 156	0.2 + 152	4	2 "	
2934	P*R31 SR	C	0.2 + 153	0.2 + 151	2	2 "	
2935	P AL/62	C	0.2 + 162	0.2 + 159	3	1 1/2"	
2936	U AL/RC	T	0.2 + 156	0.2 + 152	4	1 "	25 30
2937	P R31 NR	C	0.2 + 150	0.2 + 147	2	2 "	
2938	U R31 NR	C	0.2 + 154	0.2 + 150	4	2 1/4"	25 30
2939	U R31 SR	C	0.2 + 151	0.2 + 148	3	2 1/4"	25 30
2940	P RC/62	C	0.2 + 138	0.2 + 130	7	2 "	
2941	U RC/62	C	0.2 + 163	0.2 + 136	16	2 3/8"	10 15
2942	P*W GA	C	0.2 + 105	0.2 + 92	13	1 1/4"	
2943	U W GA	C	0.2 + 94	0.2 + 88	5	1 3/8"	10 15
2944	P*W GA	C	0.2 + 88	0.2 + 86	2	1 1/4"	
2945	P RC/GA	C	0.2 + 78	0.2 + 71	7	1 5/8"	
2946	P AL/31	C	0.2 + 75	0.2 + 72	3	1 1/8"	
2947	U AL/62	C	0.2 + 76	0.2 + 68	8	2 1/8"	25 30
2948	P*AL/62	C	0.2 + 77	0.2 + 66	3	1 3/4"	
2949	P RC/GA	C	0.2 + 58	0.2 + 51	5	1 1/2"	
2950	P W GA	C	0.2 + 64	0.2 + 33	22	1 "	
2951	U DS SPD	C	0.1 + 466	0.1 + 49	418		38 38

Subdivision: SHERBROOKE (MM&A) End of Split Split 0 totals
 From Mp: 45.00 To Mp: 0.01

Priority defects for this Split

W GA	= 166	SPXLV	= 99	RC/20	= 79	D ELV	= 10
S22 SR	= 9	RC/GA	= 11	R31 SR	= 14	RC/62	= 32
S22 NR	= 16	RC/55	= 6	R31 NR	= 14	AL/31	= 8
AL/62	= 3	RV ELV	= 5	OV ELV	= 1	AE	= 8

Total Priority defects for this Split: 481

Urgent defects for this Split

W GA	= 3	SPXLV	= 23	D ELV	= 1	N GA	= 2
R31 SR	= 3	RC/62	= 10	RC/55	= 4	R31 NR	= 4
DS SPD	= 2	AL/31	= 2	AL/62	= 1	RV ELV	= 2
RRXL	= 1	S62 NR	= 1	AL/RC	= 1		

Total Urgent defects for this Split: 60

DEF NO.	DEF P/U NAME	T/B C/E	FROM MLGE/FT	TO MLG/FT	LENGTH FT	MAX VAL	SPEED FRT/PAS
---------	--------------	---------	--------------	-----------	-----------	---------	---------------

Total Defects(PRIORITY and URGENT) for this Split:
 Total Defects = 541 Average Defects per Mile = 12.03
 Gauge OVER 1/2 inch: 19734 FT
 Gauge PRIORITY Defect Total: 3106 FT/ 177
 Gauge URGENT Defect Total: 63 FT/ 5
 Gauge RELATED Defects U and P (TOTAL): = 182
 Surface RELATED Defects U and P (TOTAL): = 61
 X-level RELATED Defects U and P (TOTAL): = 284
 Split Index Surf Rough: 47
 Split Index Crosslevel: 12

Appendix B: UMLER Data of Sample Tank Cars

Umler Equipment Management Information System

[Display Unit Report](#)

Equipment ID: TILX0000316547

Equipment Group: TANK

Date and Time: 07/13/2013 - 11:17:21 AM EDT

Flags Legend

Mandatory Value	●
ETC-Gen	▲
Rating	■

General

Element Name	ID	Flags	DB Value	Formatted Value	Conflict
Status Code	USCD	●	A	A - ACTIVE	
Mechanical Designation	UMMD	●▲	T	T - Tank	
Equipment Type Code	UMET		T108	T108	
Built Date	BLDT	●■	Confidential	Confidential	
Tank Built Date	A298		Confidential	Confidential	
Orig Cert of Constr Nbr	A183	●	Confidential	Confidential	
Rebuilt / ILS Date	RBDT		Confidential	Confidential	
Rebuilt Flag	RBFL		Confidential	Confidential	
Owner	UMOW	●	TILX	TILX	
Lessee	LESE				
Maintenance Party	MNPT		TILX	TILX	
Mark Owner Category	B201		B	B - US Private	
Prior Equipment ID	PRID				
Last Update Date	B122		20120319	03/19/2012	
Equipment Add Date	B082		20110628	06/28/2011	
Status Change Reason	USCR		M	M - Movement	
Status Change Date	USCT		20120103	01/03/2012	
Extended Service	A096	●	E	E - Built new from July 1,1974, Qualified for 50 Years Service	
End of Service Date	B078		Confidential	Confidential	
Equipment Identification	EINN		0009686431	0009686431	
EIN Duplication Flag	B074				
Info Conflict Status	B355				
Conflict Status	B050	■			
Date of Original Conflict	B053				
Next Conflict Status	B135				
Notice Indicator	B137				
Conflict Status Next Date	B062				
Rate indicator	A070	■	2	2 - Private Mileage Rate	
Private Zero Rate	B150	■			
First Movement Date	USAT		20120102	01/02/2012	
Equipment Add Company	B063				
Registration Reason	B174		N	N - New	
Restencil Program Ind	B177				

Weight

Element Name	ID	Flags	DB Value	Formatted Value	Conflict
Gross Rail Load/Weight	A266	●■	263000	263000 lb	
Tare Weight	A259	●	66400	66400 lb	
Load Limit	LDLT	●■	196600	196600 lb	
Weighing Status	A289	●	A	A - Actual	
Weighing Date	A288		20111230	12/30/2011	
Gallorage Capacity	A297	▲	30200	30200 usgl	
Star Code	A247	■			
Qual for Inc GRL	B344				
Commodity Load Restrict	B343				

Dimension

Element Name	ID	Flags	DB Value	Formatted Value	Conflict
Plate Code	A046	●■	C	C - Plate Code C	
Outside Length	OSLG	●■	713	59 ft 5 in	
Outside Extreme Width	A186	●■	128	10 ft 8 in	
Outside Extreme Height	A185	●■	186	15 ft 6 in	
Outside Height Extr Width	A187	●■	98	8 ft 2 in	
Truck Center Length	A276	■	550	45 ft 10 in	

Specification

Element Name	ID	Flags	DB Value	Formatted Value	Conflict
--------------	----	-------	----------	-----------------	----------

Page 1 of 4

RAILINC Umler		Equipment Management Information System			
Truck Count	B256		2	2	
Axle Count	A024	●	4	4	
Wheel Bearing Type	B191	●	R	R - Roller	
Bearing Shielded from HBD	B021		Y	Y - Yes	
Brake Shoe Type	B026	●	H	H - High Friction Composite	
CC Side Bearing Type	A146		LC	LC - Long Travel Constant Contact	
Empty/Load Device Eqpd	B075		Y	Y - Yes	
High Speed Design	B109				
Remote Monitoring Device	B176				
AEI High Temperature Tag	B006				
Compartment Count	A052	●	1	1	
Connected Unit Count	A020	●			
Intermediate Conn Style	B115				
Operating Brakes	A182				
ECP Brake Type	B327				
ECP Brake Builder	B328				
Equipment Builder	A035		TRIN	TRIN - Trinity	
Builder Lot Code	B030		Confidential	Confidential	
Built Country	B031		Confidential	Confidential	
Rebuilt Country	B170				
FRA Reflectorization	B096				
Tank Major Class	B207	●	10	10 - General Service Carbon Steel Tank Welded or Riveted Includes Rubber Lined	
Design Shipping Cont Spec	A072		111A100W1	111A100W1 - DOT 111A100W1	
Stenciled Shipping Spec	A237	●	111A100W1	111A100W1 - Major Class 10/18 - DOT 111A100W1	
Stub Sill Design Type	A251		TRN023	TRN023 - TRN023 Stub Sill Design	
Tank Lining Material	A315				
Tank Head Thickness	A255		0.4375	0.4375 9.9999 in	
Tank Head Mat Spec	A254	●	51670	51670 - ASTM A516, Gr. 70	
Tank Head Material Norm	B203		N	N - No	
Tank Shell Mat Spec	A257	●	128B	128B - AAR TC128, Gr. B	
Tank Shell Thickness	A258		0.4375	0.4375 9.9999 in	
TankShell Material Norm	B208		N	N - No	
Coil Material	X111				
Coils Exterior/Interior	X109				
Head Protection Thickness	B105				
Head Protection Type	A118		U	U - Unequipped	
Tank Jacket Material	B204				
Insulation Type	A142				
Insulation Thickness	B259				
Bottom Outlet/Fitting Typ	A308	●	B	B - Bottom Outlet	
Bottom Outlet Count	B142		1	1	
Bottom Fitting Protection	A153		A	A - Level A > 1" Protusion	
Top Fittings Protection	A264	●	Y	Y - Equipped	
Safety Relief Device Cnt	A181		1	1	
Safety Relief Device Type	A230	●	V	V - Valve	
Safety Vent w/Surge Prot	A231	●	N	N - No	
PWHT Not Reworked	B280				
PWHT Re-stress Relieved	B279				
Year Tank Qualified	B240				
Tank Qualification Due	B241				
Thickness Qualified Year	B246				
Thickness Qualified Due	B247				
Service Equip Qualified	B242				
Service Equipment Due	B243				
Pressure Relief Qualified	B244				
Pressure Relief Due	B245				

Cost					
Element Name	ID	Flags	DB Value	Formatted Value	Conflict
Original Cost	A184		Confidential	Confidential	
Ledger Value	A150		Confidential	Confidential	
Total A&B	A003		Confidential	Confidential	

RAILINC Umler		Equipment Management Information System					
Ind for Pos/Neg Total A&B	A128	Confidential	Confidential				
CarManagement							
Element Name	ID	Flags	DB Value	Formatted Value	Conflict		
Pool Number	P001		0000000	0000000			
Pool Control	TCPC						
User Routing Instructions	TCUR						
Umler Transportation Code	TCOD						
Transportation Cond Code	TCCD						
Mechanical Restriction	TCME						
Mech Restriction Reason	TCMR						
Sys Gen Routing Inst	TCGR	■					
Train Service							
Element Name	ID	Flags	DB Value	Formatted Value	Conflict		
286K Aprvd COC/FRA Waiver	B098						
Restricted Speed Empty	B180						
Restricted Speed Loaded	B181						
Shove car to rest	B189						
Shove adj. car to rest	B188						
Train Position Sensitive	B211						
End of Train Only	B277						
Check trailing tonnage	B044						
Curve Negotiate Exceptn	B178						
Miscellaneous							
Element Name	ID	Flags	DB Value	Formatted Value	Conflict		
Commercial Owner CIF	B049						
Commercial Lessee CIF	B048						
Umler Effective Date	EFDT		20110701	07/01/2011			
Inspection Due Dates							
Element Name	ID	Flags	DB Value	Formatted Value	Conflict		
ABT 12-Month Due Date	DU13		20121130	11/30/2012			
ABT 5/8-Year Due Date	DU58		20191230	12/30/2019			
Inspection Air Brake Test (ABT)							
Element Name	ID	Flags	DB Value	Formatted Value	Conflict		
Inspection Date Done	DTDN		20111130	11/30/2011			
Inspection Performer	PERF		TILX	TILX			
Inspection Reporter	REPT		TILX	TILX			
Location/SPLC	SPLC		921942000	921942000			
Inspection Reflectorization Event (REF)							
Element Name	ID	Flags	DB Value	Formatted Value	Conflict		
Inspection Date Done	DTDN		20111130	11/30/2011			
Inspection Performer	PERF		TILX	TILX			
Inspection Reporter	REPT		TILX	TILX			
Location/SPLC	SPLC		921942000	921942000			
Component Flat View							
Element Name	Loc	ID	Flags	DB Value	Formatted Value	Conflict	Comp.
Axes Spacing Distance	01	B020	● ■	70	70 - 70 Inches in		AXLESPACE
Axes Spacing Distance	02	B020	● ■	70	70 - 70 Inches in		AXLESPACE
Truck Axle Count	B	B252		2	2		TRUCK
Truck Axle Count	A	B252		2	2		TRUCK
Journal Size	B	A147	● ■	K	K - 6-1/ 2X 9		TRUCK
Journal Size	A	A147	● ■	K	K - 6-1/ 2X 9		TRUCK
Wheel Diameter	B	A294	● ■	36	36 - 36 Inches		TRUCK
Wheel Diameter	A	A294	● ■	36	36 - 36 Inches		TRUCK
Stability Device Equipped	B	B199	■				TRUCK
Stability Device Equipped	A	B199	■				TRUCK

RAILINC Umler Equipment Management Information System

Coupler Code	B	A057		SE60EE	SE60EE - Type E (Rule 16) - SE60EE		DRAFTSYS
Coupler Code	A	A057		SBE60EE	SBE60EE - Type E (Rule 16) - SBE60EE		DRAFTSYS
Coupler Style	B	B058	● ●	D	D - Double Shelf		DRAFTSYS
Coupler Style	A	B058	● ●	D	D - Double Shelf		DRAFTSYS
Inches of Travel	B	B061	●				DRAFTSYS
Inches of Travel	A	B061	●				DRAFTSYS
Draft Gear Type	B	B073	● ●	S	S - Standard		DRAFTSYS
Draft Gear Type	A	B073	● ●	S	S - Standard		DRAFTSYS

Page 4 of 4

TILX00000316547



Umler Equipment Management Information System

Display Unit Report

Equipment ID: WFIX0000130608

Equipment Group: TANK

Date and Time: 07/13/2013 - 11:18:11 AM EDT

Flags Legend

Mandatory Value	●
ETC-Gen	▲
Rating	■

General

Element Name	ID	Flags	DB Value	Formatted Value	Conflict
Status Code	USCD	●	A	A - ACTIVE	
Mechanical Designation	UMMD	●▲	T	T - Tank	
Equipment Type Code	UMET		T108	T108	
Built Date	BLDT	●■	Confidential	Confidential	
Tank Built Date	A296		Confidential	Confidential	
Orig Cert of Constr Nbr	A183	●	Confidential	Confidential	
Rebuilt / ILS Date	RBOT		Confidential	Confidential	
Rebuilt Flag	RBFL		Confidential	Confidential	
Owner	UMOW	●	FURX	FURX	
Lessee	LESE				
Maintenance Party	MNPT		FURX	FURX	
Mark Owner Category	B201		B	B - US Private	
Prior Equipment ID	PRID		TILX0000316400	TILX0000316400	
Last Update Date	B122		20130614	06/14/2013	
Equipment Add Date	B082		20120830	08/30/2012	
Status Change Reason	USCR		M	M - Movement	
Status Change Date	USCT		20120919	09/19/2012	
Extended Service	A096	●	E	E - Built new from July 1,1974, Qualified for 50 Years Service	
End of Service Date	B078		Confidential	Confidential	
Equipment Identification	EINN		0009686284	0009686284	
EIN Duplication Flag	B074				
Info Conflict Status	B355				
Conflict Status	B050				
Date of Original Conflict	B063				
Next Conflict Status	B135				
Notice Indicator	B137				
Conflict Status Next Date	B062				
Rate indicator	A070	■	2	2 - Private Mileage Rate	
Private Zero Rate	B150	■			
First Movement Date	USAT		20120919	09/19/2012	
Equipment Add Company	B083				
Registration Reason	B174		P	P - Pending Rescencil	
Rescencil Program Ind	B177				

Weight

Element Name	ID	Flags	DB Value	Formatted Value	Conflict
Gross Rail Load/Weight	A266	●■	263000	263000 lb	
Tare Weight	A259	●	66400	66400 lb	
Load Limit	LDLT	●■	196600	196600 lb	
Weighing Status	A289	●	A	A - Actual	
Weighing Date	A288		20111114	11/14/2011	
Gallorage Capacity	A297	▲	30140	30140 usgl	
Star Code	A247	■			
Qual for Inc GRL	B344				
Commodity Load Restrict	B343				


Dimension

Element Name	ID	Flags	DB Value	Formatted Value	Conflict
Plate Code	A046	●■	C	C - Plate Code C	
Outside Length	OSLG	●■	713	59 ft 5 in	
Outside Extreme Width	A186	●■	128	10 ft 8 in	
Outside Extreme Height	A185	●■	186	15 ft 6 in	
Outside Height Extr Width	A187	●	98	8 ft 2 in	
Truck Center Length	A276	■	550	45 ft 10 in	

Specification


Element Name	ID	Flags	DB Value	Formatted Value	Conflict
--------------	----	-------	----------	-----------------	----------

Page 1 of 4

 RAILINC Umler Equipment Management Information System					
Truck Count	B256		2	2	
Axle Count	A024	🔴 🟡	4	4	
Wheel Bearing Type	B191	🔴 🟡	R	R - Roller	
Bearing Shielded from HBD	B021		Y	Y - Yes	
Brake Shoe Type	B026	🔴	H	H - High Friction Composite	
CC Side Bearing Type	A146		LC	LC - Long Travel Constant Contact	
Empty/Load Device Eqpd	B075		Y	Y - Yes	
High Speed Design	B109				
Remote Monitoring Device	B176				
AEI High Temperature Tag	B006				
Compartment Count	A052	🔴 🟡	1	1	
Connected Unit Count	A020	🟡			
Intermediate Conn Style	B115				
A182					
Operating Brakes					
ECP Brake Type	B327				
ECP Brake Builder	B328				
Equipment Builder	A035		TRIN	TRIN - Trinity	
Builder Lot Code	B030		Confidential	Confidential	
Built Country	B031		Confidential	Confidential	
Rebuilt Country	B170				
FRA Reflectorization	B096				
Tank Major Class	B207	🔴 🟡	10	10 - General Service Carbon Steel Tank Welded or Riveted Includes Rubber Lined	
Design Shipping Cont Spec	A072		111A100W1	111A100W1 - DOT 111A100W1	
Stenciled Shipping Spec	A237	🔴 🟡	111A100W1	111A100W1 - Major Class 10/18 - DOT 111A100W1	
Stub Sill Design Type	A251		TRN023	TRN023 - TRN023 Stub Sill Design	
Tank Lining Material	A315				
Tank Head Thickness	A255		0.4375	0.4375 9.9999 in	
Tank Head Mat Spec	A254	🔴	51670	51670 - ASTM A516, Gr. 70	
Tank Head Material Norm	B203		N	N - No	
Tank Shell Mat Spec	A257	🔴	128B	128B - AAR TC128, Gr. B	
Tank Shell Thickness	A258		0.4375	0.4375 9.9999 in	
TankShell Material Norm	B208		N	N - No	
Coil Material	X111				
Coils Exterior/Interior	X109				
Head Protection Thickness	B105				
Head Protection Type	A118		U	U - Unequipped	
Tank Jacket Material	B204				
Insulation Type	A142				
B259					
Insulation Thickness					
Bottom Outlet/Fitting Typ	A308	🔴	B	B - Bottom Outlet	
Bottom Outlet Count	B142		1	1	
Bottom Fitting Protection	A153		A	A - Level A > 1" Protusion	
Top Fittings Protection	A264	🔴	Y	Y - Equipped	
Safety Relief Device Cnt	A181		1	1	
Safety Relief Device Type	A230	🔴	V	V - Valve	
Safety Vent w/Surge Prot	A231	🔴	N	N - No	
PWHT Not Reworked	B280				
PWHT Re-stress Relieved	B279				
Year Tank Qualified	B240		2011	2011	
Tank Qualification Due	B241		2021	2021	
Thickness Qualified Year	B246		2011	2011	
Thickness Qualified Due	B247		2021	2021	
Service Equip Qualified	B242		2011	2011	
Service Equipment Due	B243		2021	2021	
Pressure Relief Qualified	B244		2011	2011	
Pressure Relief Due	B245		2021	2021	

Cost					
Element Name	ID	Flags	DB Value	Formatted Value	Conflict
Original Cost	A184		Confidential	Confidential	
Ledger Value	A150		Confidential	Confidential	
Total A&B	A003		Confidential	Confidential	

RAILINC Umler		Equipment Management Information System					
Ind for Pos/Neg Total A&B	A128		Confidential	Confidential			
Car Management							
Element Name	ID	Flags	DB Value	Formatted Value	Conflict		
Pool Number	P001		0000000	0000000			
Pool Control	TCPC						
User Routing Instructions	TCUR						
Umler Transportation Code	TCOD						
Transportation Cond Code	TCCD						
Mechanical Restriction	TCME						
Mech Restriction Reason	TCMR						
Sys Gen Routing Inst	TCGR	■					
Train Service							
Element Name	ID	Flags	DB Value	Formatted Value	Conflict		
286K Aprvd COC/FRA Waiver	B098						
Restricted Speed Empty	B180						
Restricted Speed Loaded	B181						
Shove car to rest	B189						
Shove adj. car to rest	B188						
Train Position Sensitive	B211						
End of Train Only	B277						
Check trailing tonnage	B044						
Curve Negotiate Exceptn	B178						
Miscellaneous							
Element Name	ID	Flags	DB Value	Formatted Value	Conflict		
Commercial Owner CIF	B049						
Commercial Lessee CIF	B048						
Umler Effective Date	EFDT		20120901	09/01/2012			
Inspection Due Dates							
Element Name	ID	Flags	DB Value	Formatted Value	Conflict		
ABT 12-Month Due Date	DU13		20121108	11/08/2012			
ABT 5/8-Year Due Date	DU58		20191114	11/14/2019			
Inspection Air Brake Test (ABT)							
Element Name	ID	Flags	DB Value	Formatted Value	Conflict		
Inspection Date Done	DTDN		20111108	11/08/2011			
Inspection Performer	PERF		TILX	TILX			
Inspection Reporter	REPT		TILX	TILX			
Location/SPLC	SPLC		665393000	665393000			
Inspection Reflectorization Event (REF)							
Element Name	ID	Flags	DB Value	Formatted Value	Conflict		
Inspection Date Done	DTDN		20111108	11/08/2011			
Inspection Performer	PERF		TILX	TILX			
Inspection Reporter	REPT		TILX	TILX			
Location/SPLC	SPLC		665393000	665393000			
Component Flat View							
Element Name	Loc	ID	Flags	DB Value	Formatted Value	Conflict	Comp.
Axes Spacing Distance	01	B020	● ■	70	70 - 70 Inches in		AXLESPACE
Axes Spacing Distance	02	B020	● ■	70	70 - 70 Inches in		AXLESPACE
Truck Axle Count	B	B252		2	2		TRUCK
Truck Axle Count	A	B252		2	2		TRUCK
Journal Size	B	A147	● ■	K	K - 6-1/ 2X 9		TRUCK
Journal Size	A	A147	● ■	K	K - 6-1/ 2X 9		TRUCK
Wheel Diameter	B	A294	● ■	36	36 - 36 Inches		TRUCK
Wheel Diameter	A	A294	● ■	36	36 - 36 Inches		TRUCK
Stability Device Equipped	B	B199	■				TRUCK
Stability Device Equipped	A	B199	■				TRUCK

 RAILINC Umler Equipment Management Information System						
Coupler Code	B	A057		SE60EE	SE60EE - Type E (Rule 16) - SE60EE	DRAFTSYS
Coupler Code	A	A057		SBE60EE	SBE60EE - Type E (Rule 16) - SBE60EE	DRAFTSYS
Coupler Style	B	B058	● ●	D	D - Double Shelf	DRAFTSYS
Coupler Style	A	B058	● ●	D	D - Double Shelf	DRAFTSYS
Inches of Travel	B	B061	●			DRAFTSYS
Inches of Travel	A	B061	●			DRAFTSYS
Draft Gear Type	B	B073	● ●	S	S - Standard	DRAFTSYS
Draft Gear Type	A	B073	● ●	S	S - Standard	DRAFTSYS

WFIX00000130608

Page 4 of 4

Appendix C: Summary of Vampire Simulation Results

Vampire Simulation Results for Lac-Megantic Investigation R13D0054 LP188_2013							
Summarised from the statistic data files by TRRSI enclosed in the report							
Statistics between 2180 and 2200 feet centered around the POD at 2189 feet							
Wheel Dynamic Vertical Force excludes the static load /Wheel Total Vertical Force includes the static load							
Case	Simulation Condition	Wheel L/V Ratio					
		left			right		
		Mean	Min	Max	Mean	Min	Max
1	MeasuredTrack_9DegF100V65	0.443	-0.011	0.744	0.031	-0.264	0.202
2	MeasuredTrack_1p26DegF100V65	0.325	0.034	0.509	0.041	-0.255	0.143
3	MeasuredTrack_NoForceV65	0.305	0.046	0.454	0.043	-0.265	0.17
4	MeasuredTrack_9DegF100V30	0.227	0.087	0.34	0.053	-0.221	0.231
5	IdealCurve_9DegF100V65	0.394	0.261	0.4	0.056	-0.247	0.156
6	IdealCurve_1p26DegF100V65	0.28	0.173	0.307	0.127	-0.246	0.141
7	IdealCurve_NoForceV65	0.248	0.156	0.289	0.136	-0.234	0.163
8	TrackGeomOnly_NoCurve_NoFV65	0.246	-0.22	0.393	0.18	-0.071	0.347
Wheel Loading Percentage							
		left			right		
		Mean	Min	Max	Mean	Min	Max
1	MeasuredTrack_9DegF100V65	158.503	76.878	290.572	14.908	-1.778	53.349
2	MeasuredTrack_1p26DegF100V65	161.284	51.589	380.029	6.747	-0.546	35.077
3	MeasuredTrack_NoForceV65	157.755	54.577	369.397	8.605	-0.886	37.482
4	MeasuredTrack_9DegF100V30	122.976	95.499	148.346	63.562	55.215	95.68
5	IdealCurve_9DegF100V65	184.191	177.482	198.663	4.796	-0.006	25.552
6	IdealCurve_1p26DegF100V65	170.086	154.565	191.782	19.047	9.754	43.905
7	IdealCurve_NoForceV65	161.768	147.092	184.261	26.968	16.821	52.898
8	TrackGeomOnly_NoCurve_NoFV65	61.518	26.489	129.754	77.98	21.633	151.34
Wheel Lateral Force (lb)							
		left			right		
		Mean	Min	Max	Mean	Min	Max
1	MeasuredTrack_9DegF100V65	23163.21	-100	47965.25	463.734	-3200.24	2632.418
2	MeasuredTrack_1p26DegF100V65	17463.58	1673.737	36081.43	181.313	-2220.86	1061.283
3	MeasuredTrack_NoForceV65	15862.15	2305.581	29870.83	147.365	-2554.59	1161.585
4	MeasuredTrack_9DegF100V30	9734.616	3431.621	15345.09	1100.113	-5006.37	4492.36
5	IdealCurve_9DegF100V65	23769.11	14832.61	24541.44	212.118	-1487.6	692.12
6	IdealCurve_1p26DegF100V65	15536.5	8564.287	17662.48	756.386	-2666.28	1410.841
7	IdealCurve_NoForceV65	13505.47	7356.717	16601.94	1203.131	-2861.18	2103.874
8	TrackGeomOnly_NoCurve_NoFV65	5671.599	-4500.8	12609.63	4665.714	-2311.09	14740.124
Wheel Dynamic Vertical Force (lb)							
		left			right		
		Mean	Min	Max	Mean	Min	Max
1	MeasuredTrack_9DegF100V65	-18721.1	-60983.1	7399.071	27229.35	14928.22	32569.002
2	MeasuredTrack_1p26DegF100V65	-19611	-89609.2	15491.37	29840.9	20775.43	32174.758
3	MeasuredTrack_NoForceV65	-18481.6	-86207	14535.39	29246.42	20005.74	32283.424
4	MeasuredTrack_9DegF100V30	-7370.56	-15470.8	1440.268	11660.07	1382.376	14331.324
5	IdealCurve_9DegF100V65	-26941.2	-31572.2	-24794.4	30465.19	23823.52	32001.982
6	IdealCurve_1p26DegF100V65	-22427.6	-29370.4	-17460.7	25904.97	17950.31	28878.672
7	IdealCurve_NoForceV65	-19765.8	-26963.6	-15069.3	23370.1	15072.71	26617.145
8	TrackGeomOnly_NoCurve_NoFV65	12314.31	-9521.43	23523.48	7046.523	-16428.8	25077.584

		Wheel Total Vertical Force (lb)					
		left			right		
		Mean	Min	Max	Mean	Min	Max
1	MeasuredTrack_9DegF100V65	56592.61	24600.93	92983.15	10778.7	-569	17071.785
2	MeasuredTrack_1p26DegF100V65	56597.05	16508.63	121609.2	6397.035	-174.757	11224.57
3	MeasuredTrack_NoForceV65	55188.41	17464.61	118207	6547.427	-283.424	11994.26
4	MeasuredTrack_9DegF100V30	41960.6	30559.73	47470.81	24300.85	17668.68	30617.623
5	IdealCurve_9DegF100V65	62422.59	56794.39	63572.18	5610.481	-1.982	8176.481
6	IdealCurve_1p26DegF100V65	57662.44	49460.73	61370.38	9158.891	3121.328	14049.687
7	IdealCurve_NoForceV65	55067.66	47069.29	58963.64	11702.36	5382.856	16927.291
8	TrackGeomOnly_NoCurve_NoFV65	23957.33	8476.52	41521.43	31824.79	6922.417	48428.82
		Axle Sum L/V Ratio					
		front			rear		
		Mean	Min	Max	Mean	Min	Max
1	MeasuredTrack_9DegF100V65	0.454	0.018	0.729	0.509	0.158	0.742
2	MeasuredTrack_1p26DegF100V65	0.352	0.041	0.451	0.373	0.132	0.565
3	MeasuredTrack_NoForceV65	0.323	0.045	0.419	0.406	0.202	0.578
4	MeasuredTrack_9DegF100V30	0.377	0.122	0.556	0.41	0.213	0.47
5	IdealCurve_9DegF100V65	0.417	0.287	0.495	0.621	0.319	0.646
6	IdealCurve_1p26DegF100V65	0.388	0.211	0.406	0.51	0.296	0.552
7	IdealCurve_NoForceV65	0.383	0.226	0.406	0.449	0.313	0.523
8	TrackGeomOnly_NoCurve_NoFV65	0.434	0.014	0.644	0.171	0.017	0.373
		Truck Side L/V Ratio					
		left			right		
		Mean	Min	Max	Mean	Min	Max
1	MeasuredTrack_9DegF100V65	0.705	0.038	1.123	0.448	-2.81	1.714
2	MeasuredTrack_1p26DegF100V65	0.607	0.079	1.98	0.058	-0.091	0.201
3	MeasuredTrack_NoForceV65	0.896	0.095	3.734	0.074	-0.037	0.271
4	MeasuredTrack_9DegF100V30	0.331	0.169	0.447	-0.175	-0.663	0.218
5	IdealCurve_9DegF100V65	0.465	0.434	0.483	0.056	-0.026	0.123
6	IdealCurve_1p26DegF100V65	0.356	0.308	0.369	0.192	-0.202	1.95
7	IdealCurve_NoForceV65	0.329	0.275	0.351	0.157	-1.339	0.998
8	TrackGeomOnly_NoCurve_NoFV65	-0.097	-2.328	1.381	0.263	-0.286	1.67